

OPERA DIST product

Matthew C. Hansen¹, Amy Pickens¹, and Zhen Song¹

¹ University of Maryland, Department of Geographical Sciences, Global Land Analysis and Discovery (GLAD) laboratory

Corresponding Author(s): Amy Pickens (ahudson2@umd.edu)

Key Points:

7 **Abstract**

8 The earth's land surface is continually changing due to natural seasonal and interannual cycles, to direct
9 human action, and to changing climate. Land disturbance outside of the natural cycle impacts habitats,
10 climate, hydrology, food supply, and other critical systems. Improved understanding and monitoring of
11 disturbances can provide tools to land managers as well as aid scientific investigation of processes. Here, we
12 introduce a global system, DIST-ALERT, that flags all vegetation cover loss relative to its near-term historical
13 range. With a median revisit rate of <2 days, Harmonized Landsat Sentinel-2 (HLS) imagery provides the
14 highest cadence medium spatial resolution data set available and an ideal data source for monitoring the
15 earth's surface. The vegetation fraction of each new HLS observation is estimated per pixel and compared to
16 the last 3 years within a 31-day window surrounding the date of observation. Vegetation fractions less than
17 the baseline minimum are flagged as disturbance and tracked through subsequent observations to build or
18 decrease confidence. The system is agnostic to vegetation type and to resulting land cover, requiring further
19 analysis for many applications. In addition to vegetation loss, there is a secondary disturbance detection
20 algorithm based on spectral anomalies relative to the same baseline. This general disturbance detection is
21 intended to capture all kinds of other land changes including crop extensification or lava flows. Along with
22 DIST-ALERT, annual summaries of alerts are generated (DIST-ANN) to facilitate downstream science
23 through the production of synoptic annual records of global land disturbance.

24 **Plain Language Summary**

25 Human activity alters the land surface as we seek to produce fuel, food, fiber, and dwelling space for
26 expanding human populations and associated economic growth. Such changes impact the functioning of
27 natural systems, sometimes replacing them wholesale through the expansion of cities, croplands, mines, and
28 other land uses. Climate change may also impact the seasonal and interannual patterns of vegetation, altering
29 the cycles of plant growth and decay. A better understanding of these changes will aid in the scientific study
30 of their impacts on the Earth system and provide information for improved management of land resources.
31 Satellite remote sensing provides a unique opportunity to monitor these changes at scale almost as they
32 happen. This task is already being done for tropical forests. Here we extend the idea to the entire Earth land
33 surface for all vegetation with a new system: DIST-ALERT. All kinds of vegetation loss are mapped and
34 tracked through time to build or decrease confidence of change based on the severity and duration. Also,
35 anything that looks different in the current observation compared to a baseline is marked and evaluated in the
36 subsequent observations. The whole earth is imaged every 1-5 days and the maps are updated daily, though
37 cloud cover blocks some regions from being analyzed as frequently. All of the disturbance alerts from a year
38 are summarized within an annual product, DIST-ANN. Results will reflect the balance of direct and indirect
39 human impacts in the pursuit of development with the maintenance of natural systems.

40 **Version Description**

41 This is the ATBD for DIST-ALERT and DIST-ANN v1 products released March, 2024.

42 **1. Introduction**

43 Land disturbance represents a host of dynamics that impact the earth system and may be due to human-
44 induced or natural causes. For example, urbanization impacts local climate and hydrology; deforestation is a
45 major source of carbon emissions; and drought inhibits food production. Information from earth observation
46 data on land disturbance can help managers, agencies, and governments understand and respond to land
47 changes in a timely manner. Here, we define disturbance as a loss of vegetation cover outside of near-term
48 historical variability. Vegetation cover is mapped per pixel, evaluated against a seasonal baseline to detect
49 vegetation disturbance, and then tracked through the time series. To account for land disturbances unrelated
50 to vegetation loss, we also include a secondary algorithm that employs a spectral distance measure. Both
51 disturbance algorithms are applied to near-real time HLS data and deliver low latency disturbance results
52 DIST-ALERT and annual summary alert DIST-ANN. Stratified random samples are employed to validate
53 DIST-ALERT and DIST-ANN. Overall accuracy for the disturbances $\geq 50\%$ of DIST-ALERT is specified to
54 exceed 80% and of DIST-ANN, 90%.

55 **2. Context/Background**

56 **2.1. Historical Perspective**

57 Transformation of the Earth's surface has increased over time, with impacts shifting from local to global
58 scales, altering the fundamental flows of chemical and energy that sustain life on the only inhabited planet we
59 know (Kates et al., 1990). Land disturbance due to human activity impacts a range of earth system functions,
60 including climate regulation, hydrologic function, biodiversity richness, and more. For example, land use
61 change accounts for 23% of total anthropogenic forcing of climate warming (Shukla et al., 2019). Direct
62 human action in the form of land use change has accounted for roughly two-thirds of all observed land
63 change over the last 30+ years (Song et al., 2018). Deforestation, agricultural intensification, urbanization
64 and other dynamics reveal an increasing appropriation of natural lands for economic use and the increasing
65 intensification of existing land uses (Foley et al., 2005). Considerable international policy effort has focused
66 on slowing tropical deforestation in an attempt to reduce carbon emissions and limit damage to forest co-
67 benefits such as the maintenance of terrestrial biodiversity, largely with little impact to date. Monitoring land
68 change is a prerequisite to measuring its impacts, both in the policy and scientific domains.

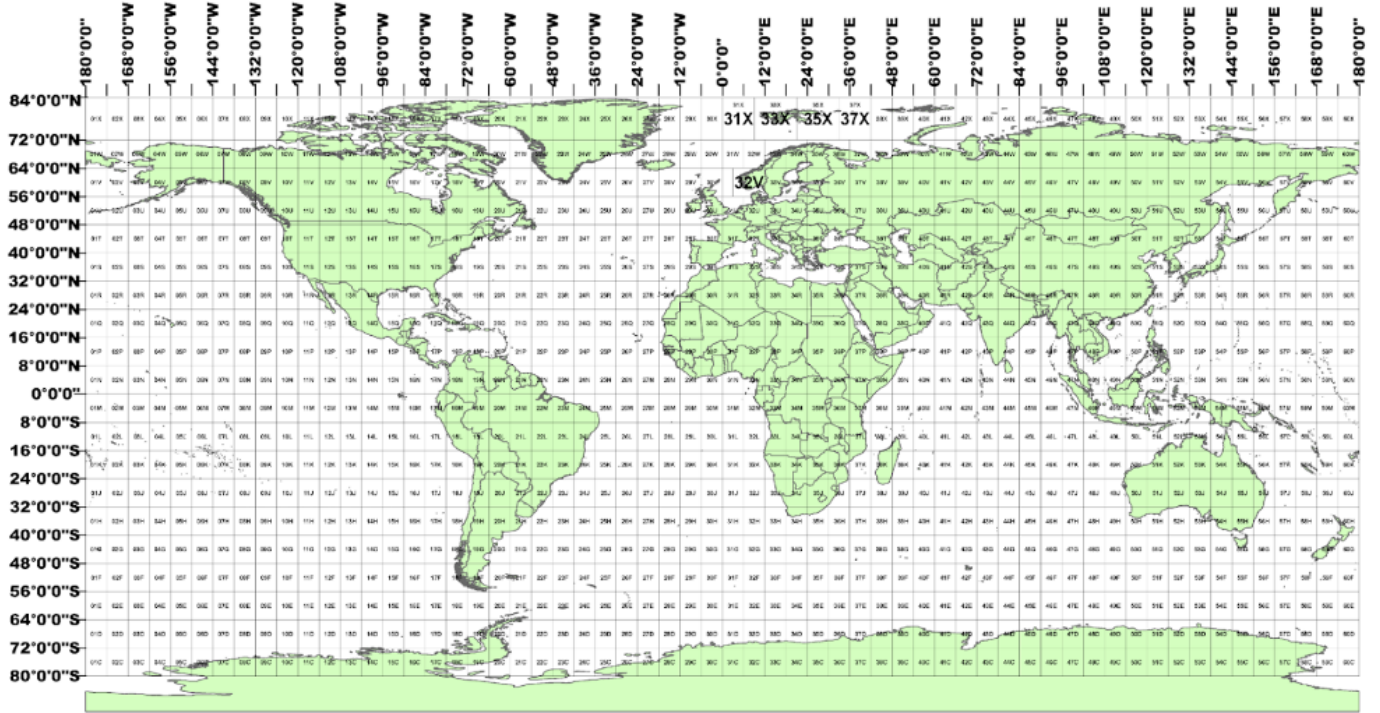
69 Climate change itself is also a driver modifying land cover and land use. Tree lines are changing, mortality
70 events increasing, droughts intensifying. Such land changes over time may become a larger fraction of the
71 overall dynamic compared to other proximate drivers of disturbance, including tipping points resulting in
72 large scale collapse of ecosystems. (Lenton et al., 2008) state that "Climate change and other human activities

73 risk triggering biosphere tipping points across a range of ecosystems and scales” and that “Researchers need
74 to improve their understanding of these observed changes in major ecosystems...” For both direct land use
75 change and more distal climate-driven land change, data on land disturbance data can offer invaluable
76 observational data and insights in support of scientific inquiries concerning global environmental change.

77 Disturbance is defined as any event that occurs outside the range of natural variability
78 (Mildrexler et al., 2009) and may be due to human-induced or natural causes. Disturbance indicates an
79 impact on land cover or land use that may result in a complete conversion or only a modification of the pre-
80 existing condition. Disturbances can be instantaneous or long-lived, limited in area or regional in scale.
81 Differentiating the limit of natural variability is a key requirement in assigning disturbance, as many
82 ecosystems and associated land covers can be highly interannually variable, as are land uses. Additionally,
83 many land covers and land uses are defined by disturbance, such as fire regimes in boreal forests, or rotations
84 in forestry land uses.

85 Disturbance is often characterized in ecological terms as events that alter ecosystem extent, structure,
86 communities, and other variables. Deforestation, mining, fire, drought and other dynamics, whether human-
87 induced or natural in cause, result in a reduction in vegetation cover with concomitant impacts on ecosystem
88 function. For this application, we focus on such dynamics and define disturbance as a loss of vegetation
89 cover outside of near-term historical variability. In this way, we modify the general definition of disturbance
90 to being a cover change of more to less vegetation cover. The presented method and associated disturbance
91 algorithm is applied in near-real time as new imagery are available, delivering low latency results to facilitate
92 land management decision-making. Annual summaries of alerts are then delivered, facilitating downstream
93 science through the production of synoptic annual records of global land disturbance.

94 The potential uses of vegetation disturbance alerts at medium spatial resolution (10-30 m from globally
95 acquired, publicly available sensing systems such as Landsat and Sentinel 2) range from enforcement to
96 management applications. Monitoring road building, logging, forest clearing for agriculture and other
97 dynamics can have added value if reported in near-real time. The DETER alerts of Brazil were critical to
98 increasing the capacities of law enforcement and land management agencies in reducing illegal deforestation
99 in the Brazilian Amazon (Nepstad et al., 2014). The deployment of such a system pan-tropically by Global
100 Forest Watch through the University of Maryland’s Global Land Analysis and Discovery (GLAD) lab, has
101 offered such possibilities to other countries. Studies have showed GLAD alerts to have been used to reduce
102 deforestation in community forests in Peru and Central Africa (Slough et al., 2021); (Moffette et al., 2021).
103 Here, we advance this approach by applying it at global scale with a continuous measure, characterizing
104 generic vegetation loss instead of only forests, and employing the highest cadence medium spatial resolution
105 (30 m) data set available, in the form of Harmonized Landsat Sentinel-2 data (HLS), as the input. The HLS
106 tiling system is shown in **Figure 1**. The integration of both medium spatial resolution systems greatly
107 enhanced the temporal resolution (2-4 day repeat) of these data, which improves alert capabilities.



108 Figure 1: The global map of tile IDs for the HLS products (same as original Sentinel-2 tiling system).

109 **3. Algorithm Description**

110 **3.1. Scientific Theory**

111 Operational disturbance alert systems can be signal or land cover theme-based. Signal-based systems use a
 112 radiometric measure, such as greenness or brightness temperature, as the primary input to the alert system,
 113 delineating change outside normal variation of these bio-geophysical variables. By comparison, theme-based
 114 alerts characterize a specific land cover change dynamic over a time series, such as forest cover loss, i.e., the
 115 removal of tree cover, or flooding, i.e., an increase in the expanse of surface water beyond the norm. As
 116 such, land cover theme-based alert systems provide a more intuitive physical meaning and a resulting ability
 117 to map and validate area estimates more easily than bio-geophysical measures.

118 Fractional vegetative cover is a theme-based measure and the basis of the OPERA Surface Disturbance
 119 (DIST) algorithm. Fractional cover estimations from satellite data have a long history, employing a host of
 120 algorithms, from simple linear endmember mixture models (Adams et al., 1995); (Settle & Drake, 1993),
 121 multiple endmember mixture models (Roberts et al., 1998), empirical modeling (DeFries et al., 1997);
 122 (Zhu & Evans, 1994), and distribution-free machine learning methods (Hansen et al., 2002). The
 123 advantages of continuous dependent variables such as percent tree or vegetation cover include improved
 124 sensitivity to change compared to categorical labels, greater flexibility for users to adjust definitions, and more
 125 realistic depictions of ecotones.

126 Operational alerts of land change have been employed in a variety of modes, ranging from illegal
127 deforestation monitoring in Brazil with the Real-Time System for Detection of Deforestation (DETER)
128 (Shimabukuro et al., 2012), to active fire monitoring with the NASA's Fire Information for Resource
129 Management System (FIRMS)(Davies et al., 2008), to food security with the Famine Early Warning System
130 (FEWS) of USAID (Ross et al., 2009). Newer products include the use of medium spatial resolution data,
131 for example Global Forest Watch's deforestation alerts (Hansen et al., 2016) made from Landsat and
132 Sentinel-2 data. To advance this capability, we will implement a global low latency alert, DIST-ALERT, and
133 an annual summary, DIST-ANN, product suite using NASA's Harmonized Landsat Sentinel-2 data (HLS)
134 (Claverie et al., 2018) as inputs. The combined capability of these Earth observing systems results in a 2-4
135 day repeat visit cadence globally (Li & Roy, 2017), facilitating the application of near-real time disturbance
136 mapping.

137 Vegetation fraction is a suitable variable for monitoring global land change. Our team has developed global
138 algorithms for mapping per pixel percent vegetation cover using MODIS and Landsat data
139 (Carroll et al., 2010); (Hansen et al., 2014); (Ying et al., 2017). Results with Landsat demonstrate the utility
140 of the measure in mapping the dynamic of vegetation loss and employing the maps to sample-based and
141 econometric methods to estimate land use outcomes/drivers and apply the measure as a leading economic
142 indicator, respectively (Ying et al., 2017); (Ying et al., 2019). Vegetation loss as a generic dynamic can
143 inform specific downstream applications from local to global scales and we will apply percent vegetation to
144 HLS time-series imagery (Claverie et al., 2018) in mapping land disturbance.

145 **3.1.1. Scientific Theory Assumptions**

146 The first assumption in monitoring land disturbance, as we have defined it, concerns disturbances that involve
147 vegetation loss. In terms of global environmental change, vegetation loss is a key indicator, whether the
148 dynamic is deforestation, desertification, overgrazing, or fire. However, a limited number of disturbance
149 dynamics do not involve vegetation loss, for example redevelopment of a commercial parcel, or lava flow
150 superposed on old lava fields. An open question is the proportion of disturbance, as defined by generic
151 surficial change events, that is omitted when targeting vegetation loss. It is the assumption that the vast
152 majority of land disturbance relevant to policy, management and science applications will be observable using
153 vegetation cover as the indicator variable. To confirm this assumption, we will add a Mahalanobis distance
154 measure to delineate generic changes outside of the vegetation cover loss theme.

155 Another assumption concerns the ability of optical time-series data to discriminate relevant vegetation loss
156 events accurately and in a timely fashion. Large conversion events, such as deforestation, have been shown
157 to be reliably characterized (Hansen et al., 2013), while modification, or degradation of land cover types, has
158 more mixed results. Conversions represent a high contrast, typically long-lived spectral change.
159 Modifications represent low contrast, often ephemeral spectral change. The manner in which we plan to add
160 signal for detecting modifications, in effect to improve contrast, is to exploit the density of the HLS time-
161 series. Repeated alert detections, even if low in contrast individually, can in concert enable accurate
162 assignment of low intensity land disturbance. As a safeguard, our product specification and definition of

163 disturbance is for 50% or greater vegetative cover loss events, or more suited for conversion than
164 modification.

165 **3.2. Mathematical Theory**

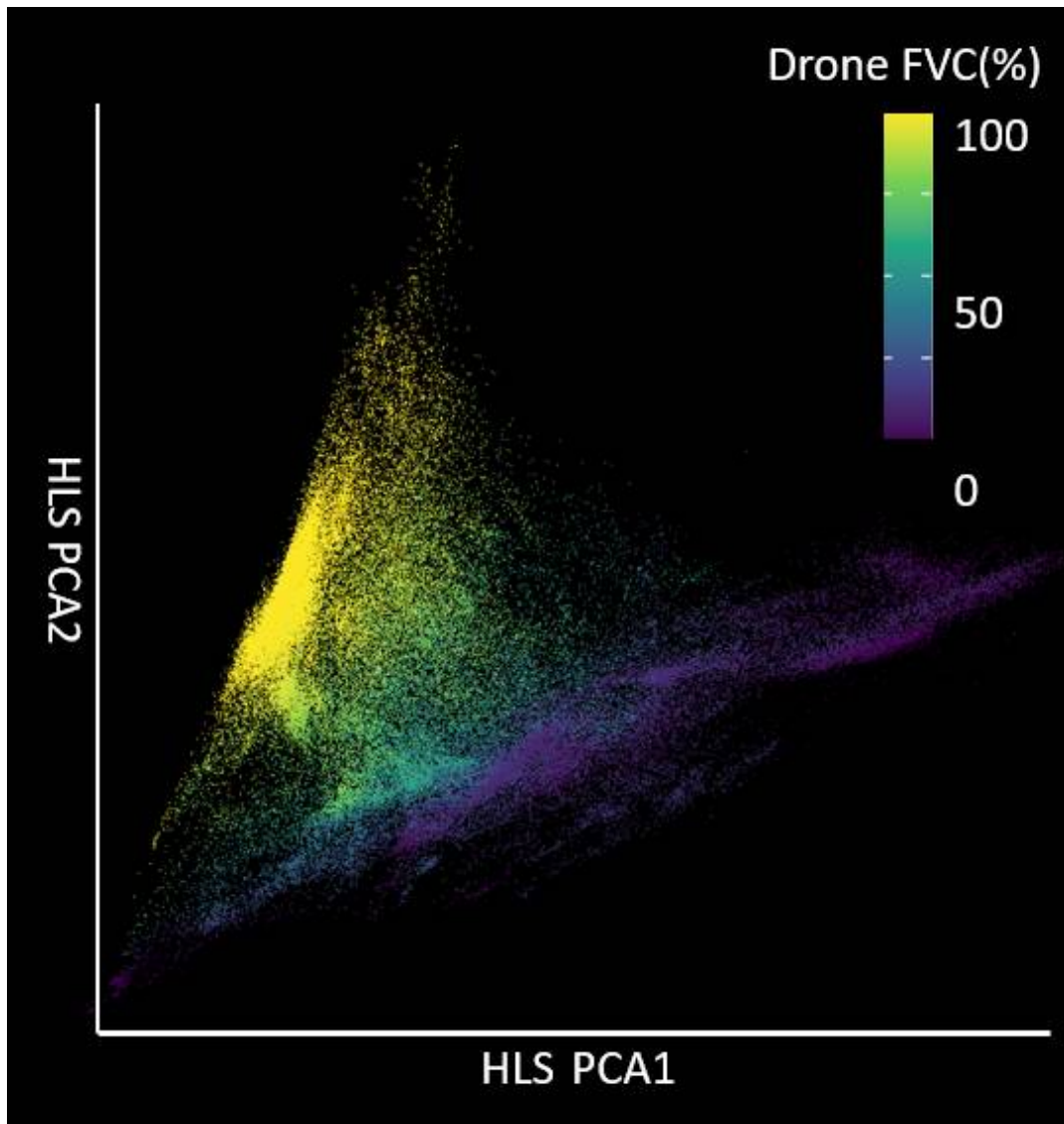
166 **Vegetation Fraction Algorithm**

167 We have been working on Vegetation Continuous Field (VCF) maps for years, including MODIS VCF
168 (Hansen et al., 2002), (Hansen et al., 2003) and Landsat-based VCF maps (Hansen et al., 2014);
169 (Ying et al., 2017). In this product, we employ 8cm drone images and K Nearest Neighbor (KNN) model to
170 characterize vegetation fraction. Our model relies on the following assumptions for successful estimation:

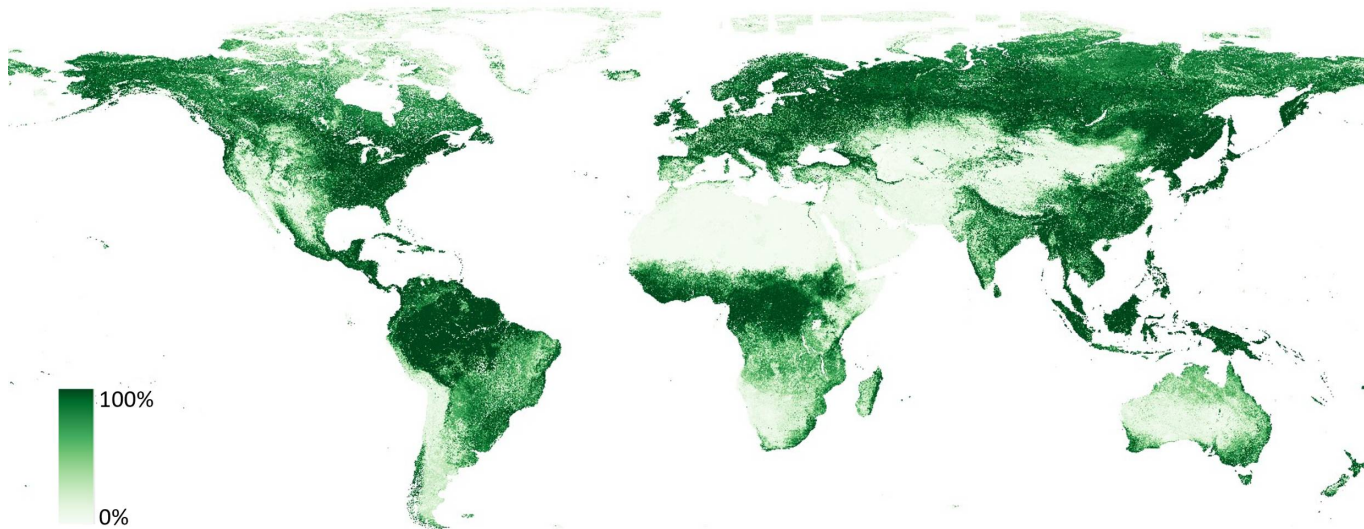
- 171 1. Consistent radiometric characterization of input imagery. The HLS time-series data feature state of the
172 practice pre-processing including surface reflectance estimation and bi-directional reflectance distribution
173 function correction, resulting in a reliable, scale set of independent variables for inputs into a turn-key
174 KNN model.
- 175 2. Accurate quality assessment flags in screening inputs. The HLS data come with a quality assessment flag
176 that must accurately screen unviable observations. No quality assessment layer is perfect, but too many
177 omission errors in terms of passing haze/cloud/smoke/shadow-impacted observation leads to errors in
178 mapping land change. However, the unprecedented density of the HLS time-series mitigates against
179 occasional errors in quality flags.

180 Given consistent spectral inputs and quality assessment, a drone data based KNN model is built to estimate
181 the per-HLS pixel vegetation fraction. Drone images were collected across different biomes at different
182 seasons, covering representative land cover and land use. NDVI was selected to calculate vegetation fraction
183 over other indices that employ additional shorter wavelength bands that are impacted by greater scattering
184 effects which we sought to avoid in a global application. A linear translation of NDVI to vegetation fraction
185 was applied for the range of 0.10 to 0.80 based on the studies of (Jiang et al., 2006),
186 (Tucker & Nicholson, 1999), and (Gitelson et al., 2002). Modifying the model to account for varying
187 illumination effects and background soil variation was not feasible, particularly for a global application. For
188 this product, the linear translation was applied to the 8cm drone NDVI values and then aggregated to 30m
189 HLS -pixel level. The averaging of these data to 30m is assumed to ameliorate less well characterized mixed
190 pixels at the 8cm scale. Then we matched the coincident clear-sky HLS data with drone images and
191 employed four bands of HLS data, including red, nir, swir 1.6 and swir 2.1 bandwidths, and drone-derived
192 vegetation fraction as the training inputs (Figure 2). Only bands that are present in both the HLS Landsat and
193 HLS Sentinel collections were included. Additionally, to avoid residual atmospheric contamination, we did
194 not employ shorter wavelength blue and green bands as independent variables in estimating vegetation
195 fraction. We converted the four HLS bands to three principal components through principal component
196 analysis and built the KNN model based on the three principal components using a K-value of 100. The
197 result is a turn-key model which can be applied to any HLS image using the aforementioned bands. The main
198 assumption of the resulting model is that the samples cover all ranges of vegetative cover and may be applied

199 to all the HLS images. A global composite can be seen in Figure 3. While many cover types require a time-
200 series for identification, whether forests or croplands, vegetation fraction can be mapped instantaneously,
201 much like water. As such, time-series of HLS observations in the form of vegetation cover can be used to
202 monitor land change.



203 Figure 2: Training data collected from drone-derived Fractional Vegetation Cover (FVC) and coincident HLS data. The
204 data is shown at the first two principle components derived from HLS red, nir, swir 1.6 and swir 2.1 bandwidths,
205 denoted as HLS PCA1 and PCA2.



206 Figure 3: Global vegetation fraction estimates from HLS data from July 2023, gap-filled by surrounding months.
207 Vegetation fraction calculated as percent vegetation cover with the KNN model derived from drone data.

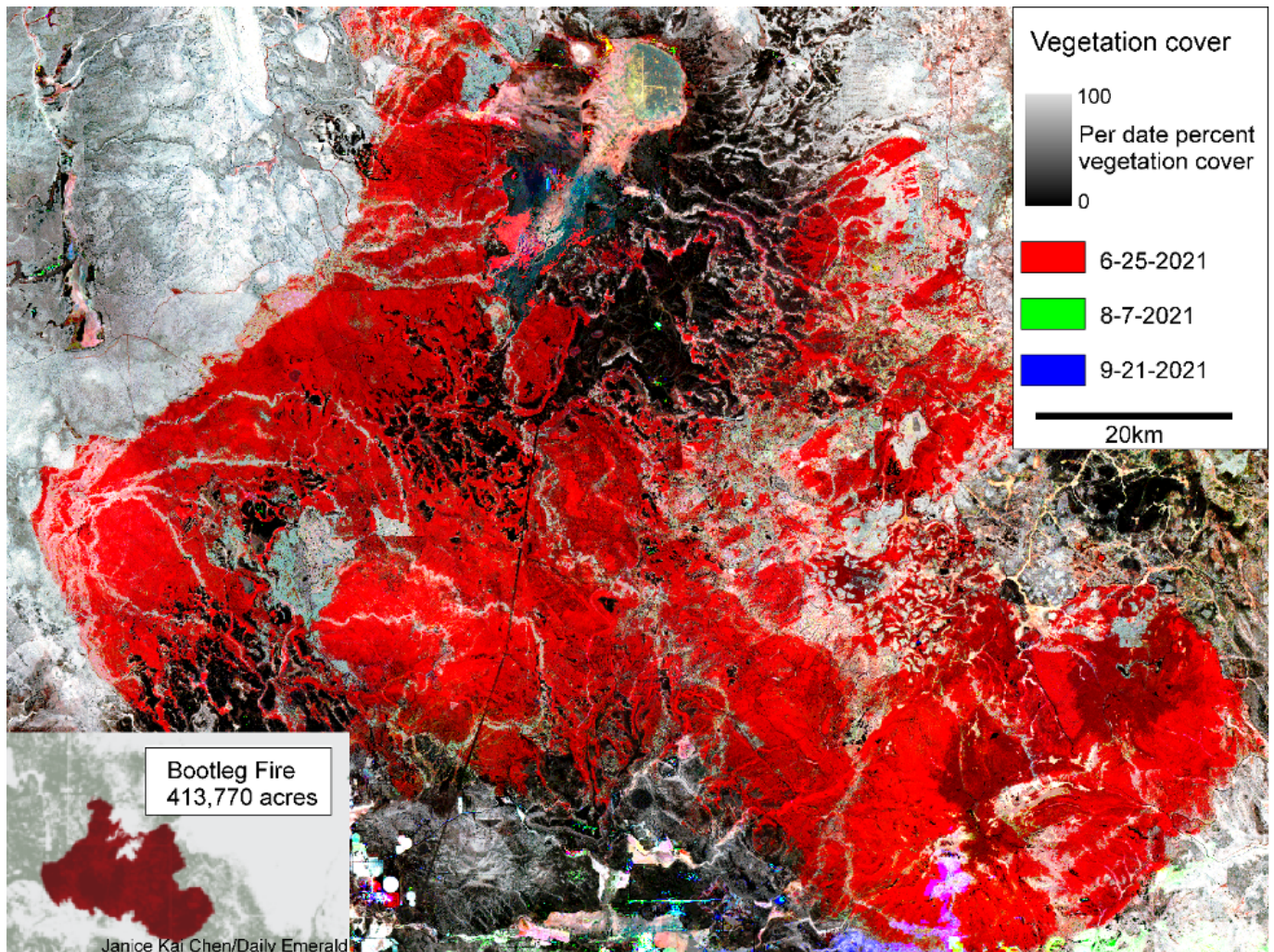
208 Vegetation Disturbance Algorithm

209 The DIST algorithm employs a vegetation cover indicator as the input variable. Vegetation cover can be
210 mapped per pixel, recording the natural phenological or managed land use dynamic of the land surface. Near-
211 term historical variation can then be used as a reference for detecting anomalous vegetative cover estimates.
212 Vegetation cover is defined as “the amount of skylight orthogonal to the surface that is intercepted by the
213 cover trait of interest” (Carroll et al., 2010) and includes all plant life over land including both woody and
214 herbaceous (i.e., non-woody) vegetation as with the MODIS VCF product (Hansen et al., 2013)
215 (MODIS VCF ATBD, n.d.). Vegetation disturbance is mapped when there is an indicated decrease in
216 vegetation cover within an HLS pixel, formally defined to be 50% vegetation cover decrease when the scene
217 is compared to the previous calendar years as in (Ying et al., 2017), though the algorithm will report a
218 continuous record of vegetation cover loss. The number of calendar years used as a reference is three years.

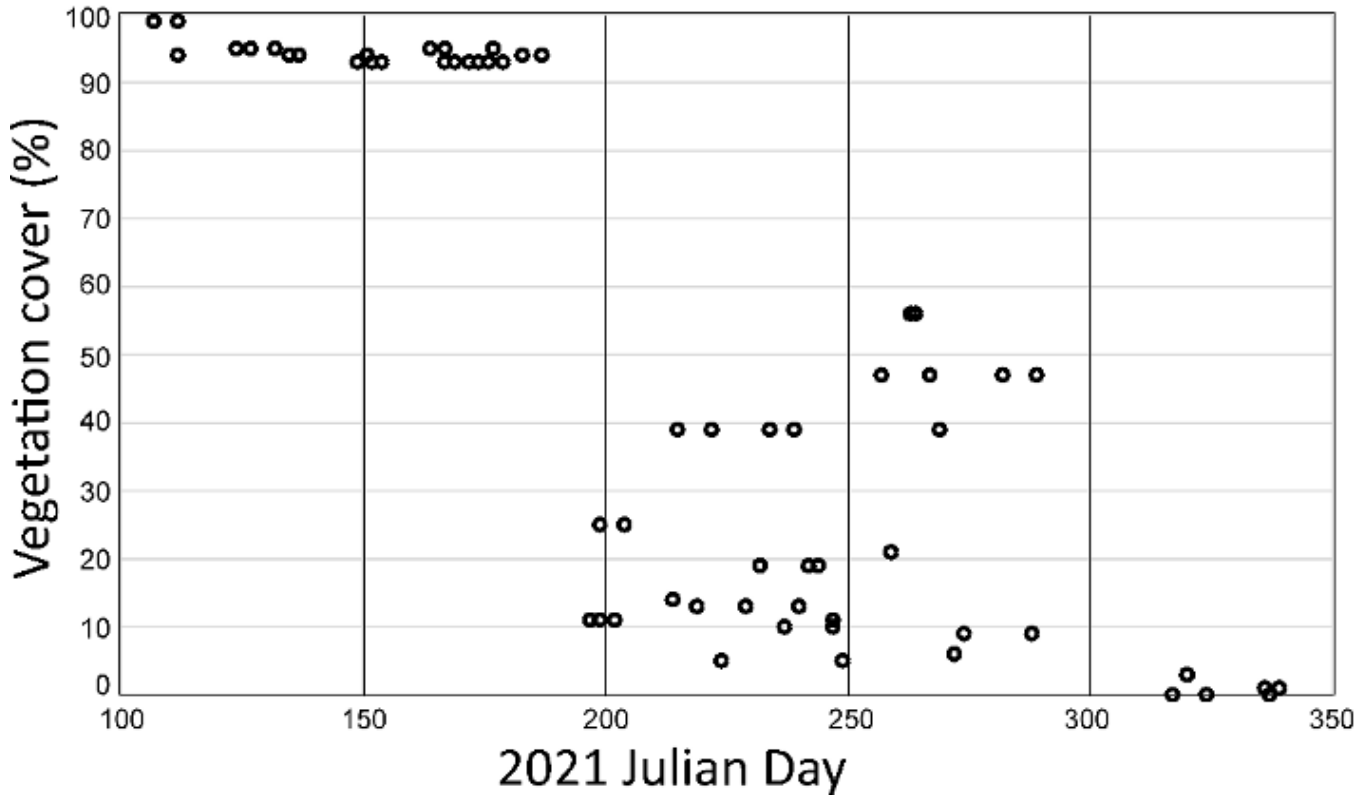
219 Applying the per scene vegetation cover model will result in a time-series of per pixel vegetation cover.
220 **Figure 4** shows three dates of HLS-derived vegetation cover over the Bootleg Fire in Oregon, USA. The
221 dates were chosen as they were cloud/smoke-free and outline the scale of the fire extent. **Figure 5** depicts a
222 time-series of vegetation cover for a pixel at the western edge of the fire, illustrating the start of the fire for
223 this pixel sometime after the morning of July 6. Disturbance, or vegetation loss, is quantified by the next
224 cloud/smoke-free image on July 16. In algorithm implementation, disturbances in vegetation cover will be
225 identified by comparing each current HLS scene to a summary of cover estimates from previous years
226 representing a lower bound of observed vegetation cover. The composite historical reference is derived from
227 the minimum vegetation fraction of all observations in the previous three years within a 31-day window
228 surrounding the calendar date of the current HLS scene. In order to capture more representative conditions, at
229 least four historical observations are required to calculate the vegetation cover anomaly. In this manner, we
230 may account for intra-annual and seasonal variation in quantifying anomalously low vegetation cover
231 conditions. Regions with high cloud frequency may always have four observations within the baseline
232 period, such as regions of humid tropical forests. In order to enable greater monitoring capacity in these

233 regions, we also employ a three-year, 12-month baseline minimum from the three previous calendar years to
234 identify areas with stable high vegetation presence. When there are not four seasonal baseline estimates
235 available and the annual baseline is $\geq 85\%$, then the annual baseline cover estimate is used as the reference
236 baseline to calculate the vegetation cover anomaly.

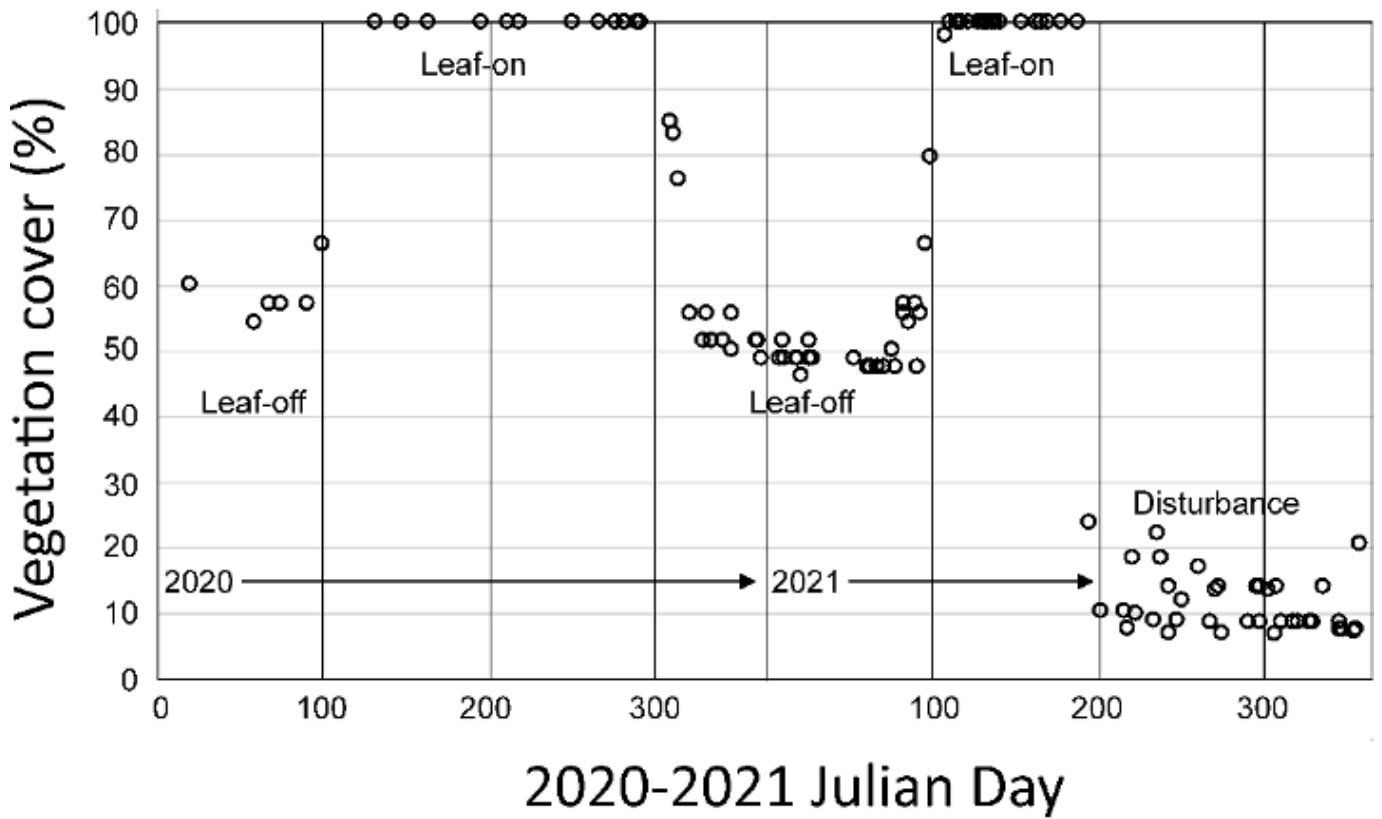
237 Strongly seasonal environments may have periods where detection of land disturbance is precluded. For
238 example, low sun angles and winter conditions will lead to fewer observations and lower vegetation contrast
239 when observed. However, the vegetation cover model is sensitive to leaf-off non-photosynthetic woody
240 cover in semi-deciduous and deciduous environments, meaning forests and woodlands will register a positive
241 leaf-off vegetative cover. This outcome is due to the fact that dense leaf-off tree cover has a similar spectral
242 signature to peak greenness transitional shrublands in semi-arid ecotones. **Figure 6** illustrates leaf-on, leaf-off
243 vegetation cover estimates as compared to a clearing event in northern Virginia, USA.



244 Figure 4: HLS-derived vegetation cover for three dates in r-g-b color composite. Red indicates vegetation loss after June
245 25, 2021. The three dates were chosen as they were cloud-free and graphically capture fire extent.

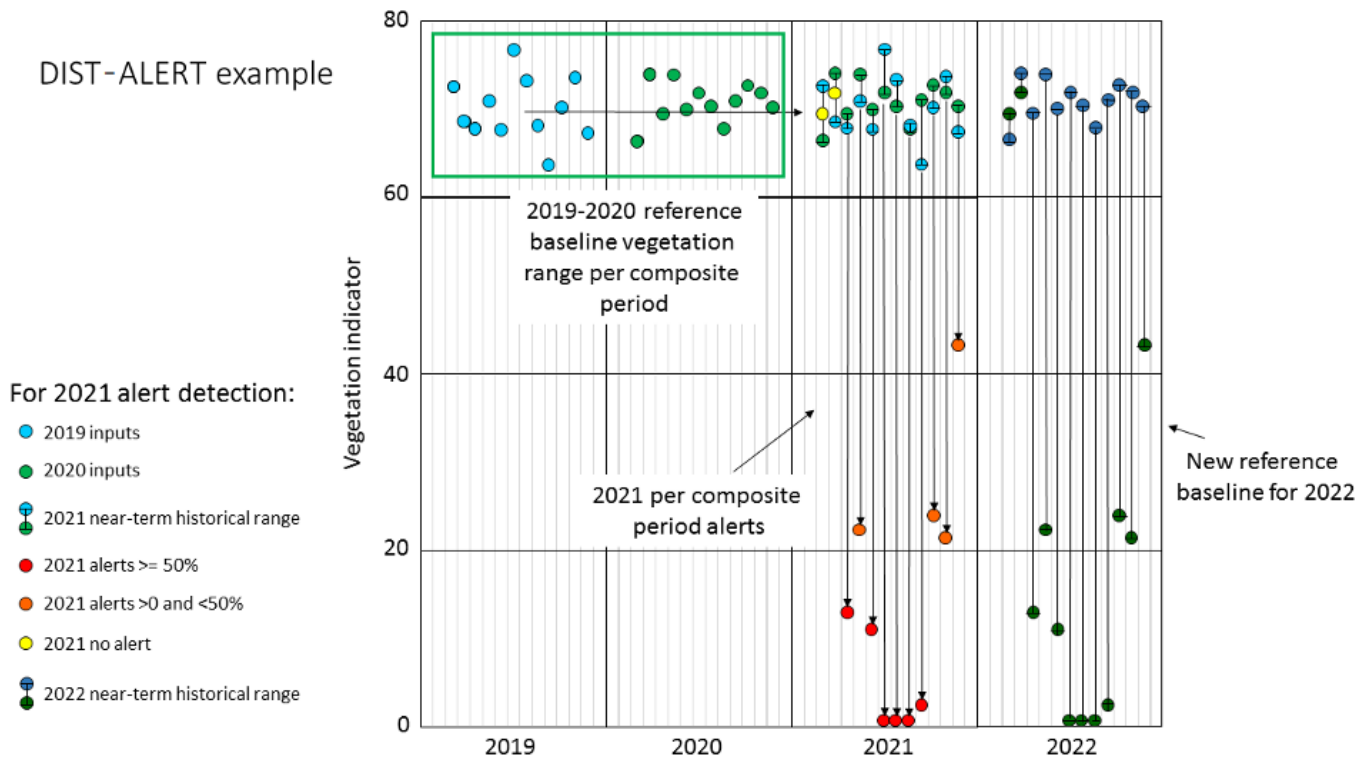


246 Figure 5: HLS-derived percent vegetation cover for fire-disturbed pixel on the western edge of the Bootleg Fire, Oregon,
247 USA. Pixel is located at 121°24'51"W, 42°38'31"N.

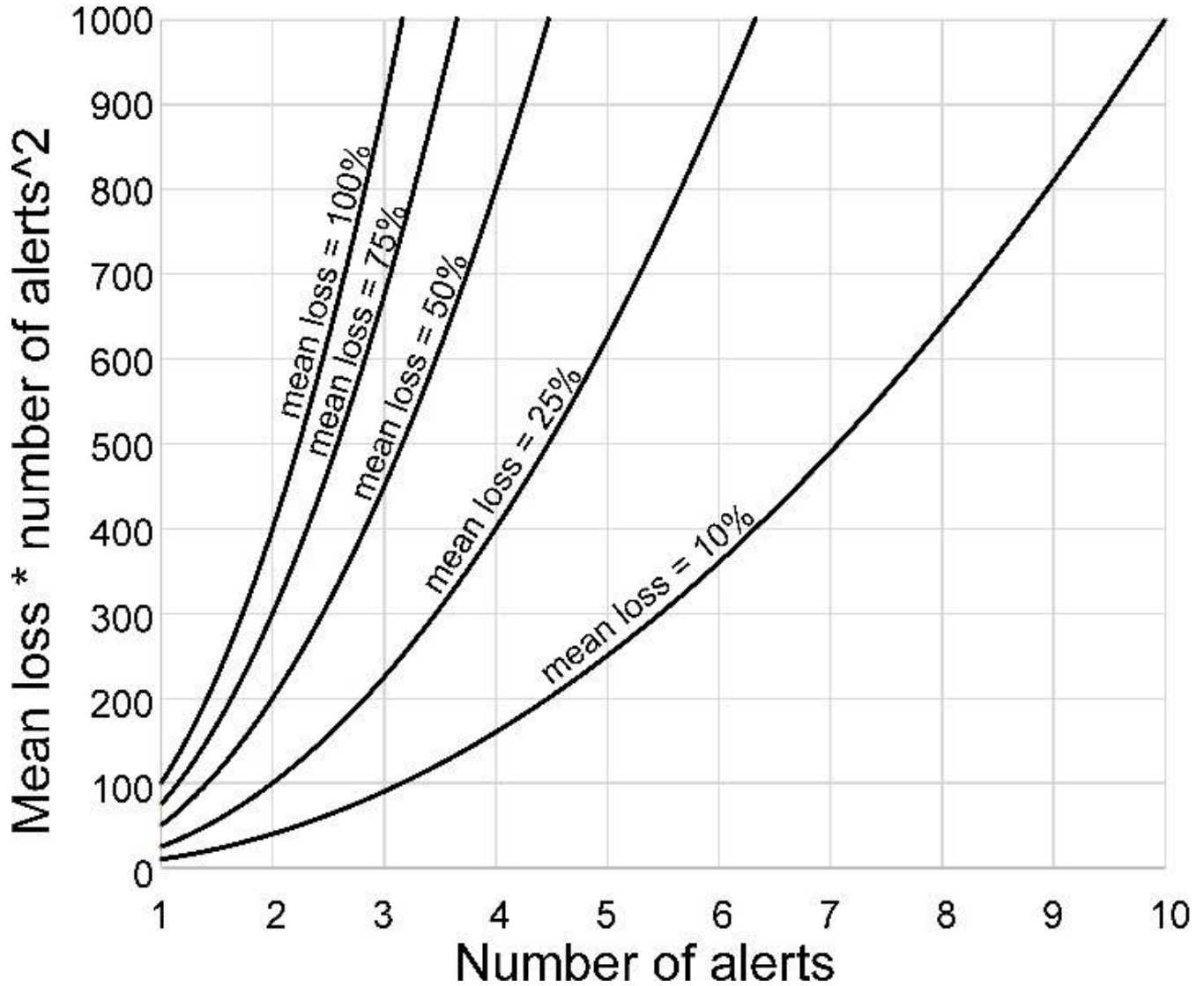


248 Figure 6: HLS time-series of vegetation cover for deciduous forest pixel in Virginia, USA, cleared between July 9th and
249 16th, 2021.

250 **Figure 7** shows an example pixel from a shrubland outside of Fort Worth, Texas, USA being converted to a
 251 residential land use. In this simplified example, two years of Landsat Analysis Ready Data are composited
 252 and the historic per-composite ranges used as a reference for the current year. Observations of the current
 253 year are compared to the range of their respective composite periods and vegetation cover estimates below
 254 the lower bounds indicate loss. The anomaly magnitude and current vegetation cover estimates are recorded.
 255 Both the magnitude and frequency of alerts will be used to integrate time-series information with repeated
 256 alert observations resulting in confirmed land disturbance assignment. Beyond confirmed status, a
 257 confidence layer which weights repeated alerts will be generated, where confidence equals the mean
 258 vegetation loss over a series of alerts multiplied by the number of alerts squared. **Figure 8** illustrates
 259 scenarios for a range of mean vegetation loss values for this measure. As the system moves forward, the
 260 reference data are updated and, in the case shown in **Figure 7**, a new range of reference vegetation cover will
 261 preclude alerts from being repeated in the following year. The full set of time-series layers, including
 262 confidence, date, and duration are listed in **Table 1**.



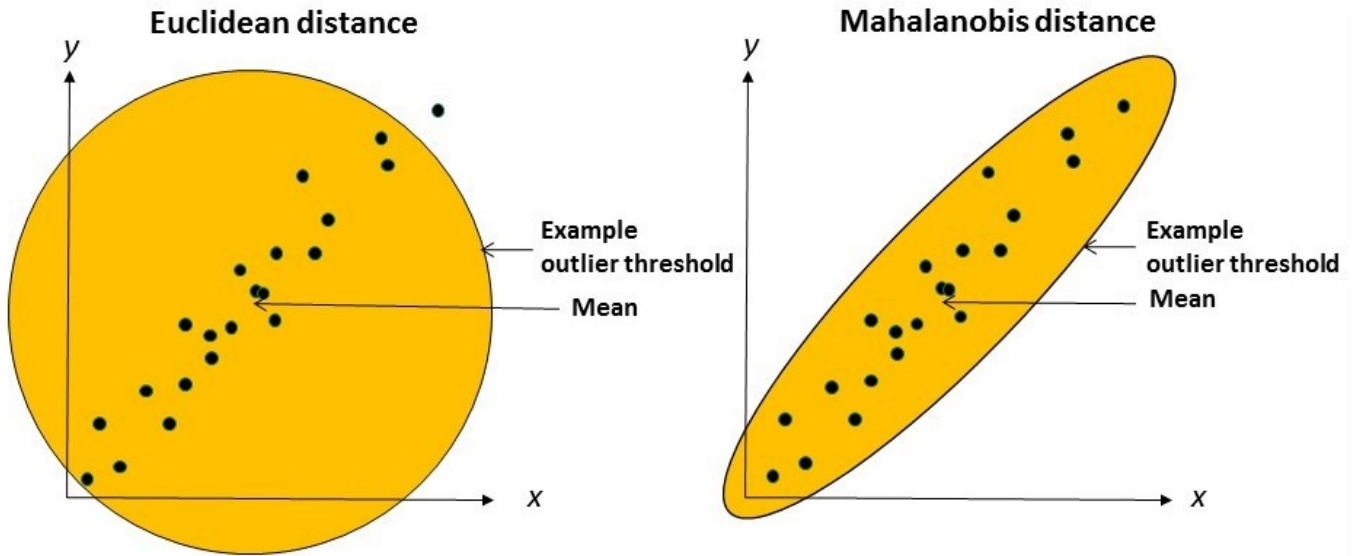
263 Figure 7: DIST-ALERT example from Analysis Ready Data Landsat observations for a sub-tropical shrubland conversion
 264 event near Fort Worth, Texas.



265 Figure 8: Confidence layer approach (y-axis) combining alert magnitude and frequency. For example a mean 10% loss
 266 for 6 alerts would have a confidence of 360.

267 Spectral Distance Secondary Algorithm

268 To account for land disturbances unrelated to vegetative cover loss, we include a secondary algorithm that
 269 employs a spectral distance measure. Near-time historical data, as with the vegetation fraction algorithm, will
 270 be used to calculate a spectral envelope that delimits a normal range of spectral variation. Current HLS
 271 spectral signatures will be compared to the normal historical range and outliers calculated. The measure
 272 chosen is Mahalanobis distance, as it accounts for co-variance in the near-term historical range, unlike
 273 Euclidean distance. **Figure 9** shows the difference between Mahalanobis and Euclidean distance in
 274 graphical form, comparing the two measures. Each pixel will have a Mahalanobis function based on
 275 historical data for the current temporal window from two or more years, as with the vegetation fraction
 276 algorithm. A minimum of six historical clear land observations are needed to calculate the baseline envelope.
 277 The function will be applied to the current red, near-infrared, and two shortwave infrared bands, again as
 278 with the vegetation fraction algorithm, and the value recorded for all valid land observations per HLS scene.
 279 Time-series layers derived from the spectral distance alerts will mimic those of the vegetation fraction model,
 280 and are listed in **Table 1**.



281 Figure 9: Graphical comparison of Euclidean and Mahalanobis spectral distance measures. Mahalanobis functions
 282 calculated from historical data, which better account for co-variance, will be applied to new observations and spectral
 283 distances from the mean recorded per HLS scene.

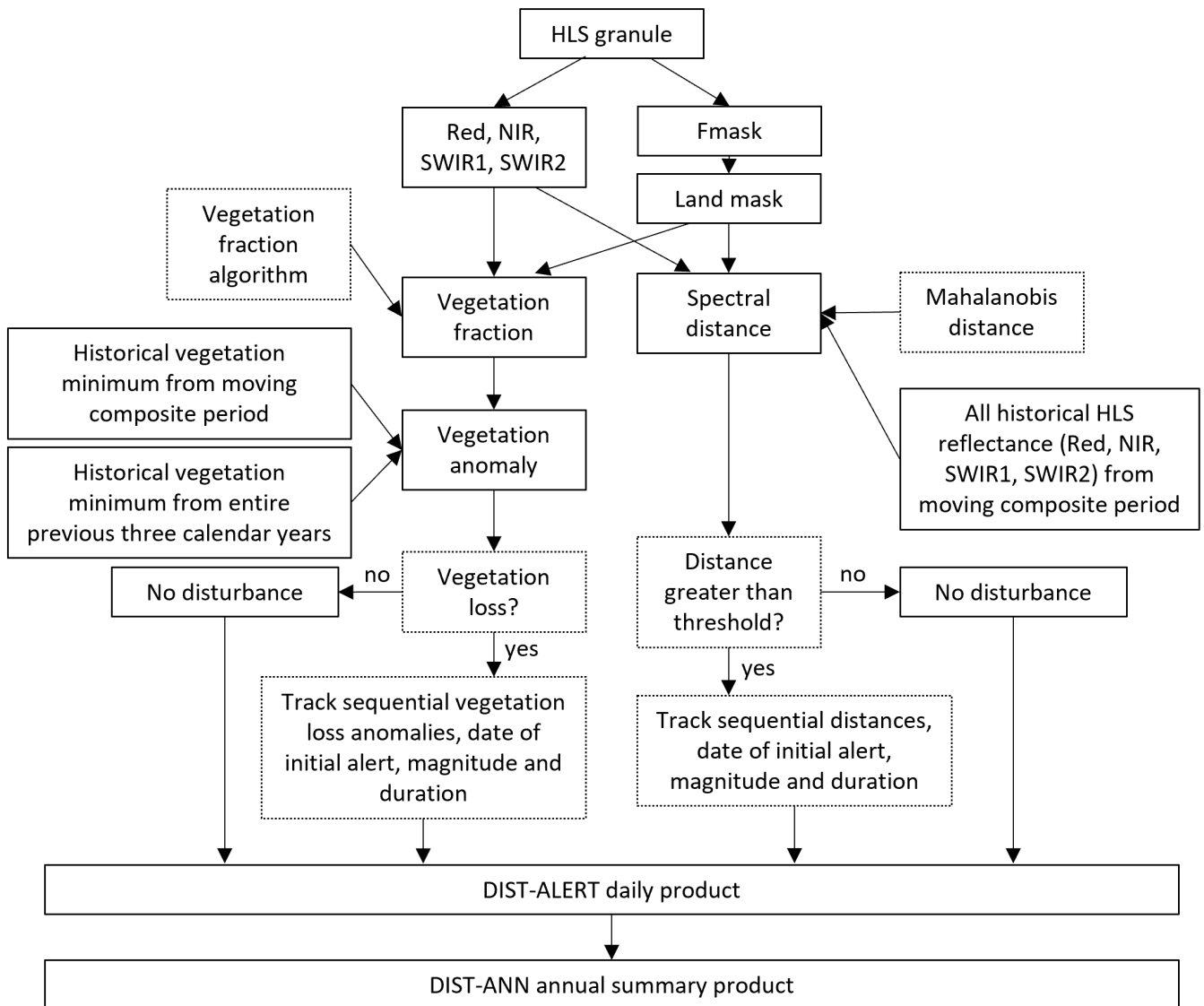
284 Algorithm Implementations

285 Two DIST products are generated with respect to their temporal relevance: a) the DIST-ALERT product
 286 capturing disturbance at the cadence of HLS sampling (median average 2.9 days for HLS (Li & Roy, 2017))
 287 and b) the DIST-ANN product summarizes changes of the DIST-ALERT products from the previous year.
 288 The date of the first disturbance is tracked within both products. Each DIST-ALERT product is associated
 289 with an HLS scene and is used to track vegetation disturbances at the temporal frequency of the input HLS
 290 dataset. The DIST-ANN tracks changes at the annual scale, aggregating changes identified in the DIST-
 291 ALERT product. **Figure 10** shows the general flow of operations and products for both algorithms.

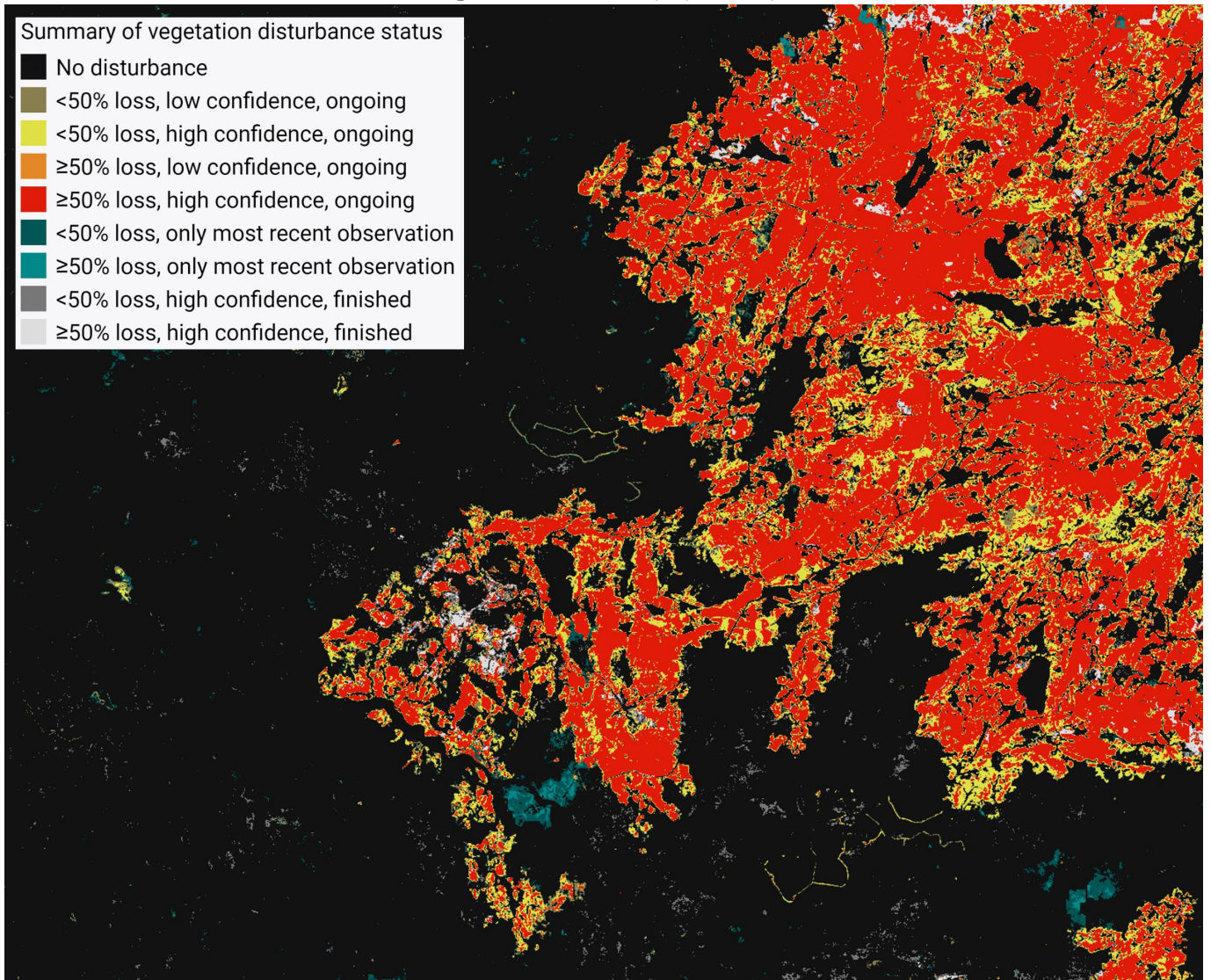
292 The DIST-ALERT product tracks disturbances from initial detection through subsequent observations to
 293 increase or decrease confidence. Disturbances identified with the vegetation loss algorithm are tracked
 294 independently from those identified with the spectral distance algorithm, but they are each monitored with a
 295 parallel set of rules. Disturbances are marked as provisional or confirmed and as low or high intensity. All
 296 disturbances begin as provisional alerts starting with the date of initial detection. Through repeated anomaly
 297 detections in subsequent observations, alerts can move to confirmed status. The precise number of valid land
 298 observations required for a confirmed status will be determined during the algorithmic calibration and are a
 299 function of both the magnitude of the anomaly and the number of anomaly detections. This confirmation will
 300 come from a variable number of HLS scenes due to invalid observations contaminated by cloud or shadow. If
 301 a pixel marked provisional disturbance has no observed loss in subsequent images, then this label will be
 302 removed and this pixel's vegetation cover will continue to be analyzed for future vegetation cover losses.
 303 Additional contextual layers are provided for disturbed pixels including: the date of initial disturbance,
 304 vegetation disturbance confidence, number of observed anomalies, and disturbance duration. An example of

305 provisional versus confirmed alerts is shown in Figure 10. For vegetation loss disturbances, pixels are also
 306 marked as low or high intensity based on whether the estimated vegetation cover loss is $\geq 50\%$. For general
 307 disturbances identified by the spectral distance algorithm, the distance threshold delineating low and high
 308 intensity will be determined during algorithm calibration.

309 In DIST-ANN, only confirmed disturbances from the associated year are reported together with the date of
 310 initial disturbance. As confirmed disturbances are determined using subsequent cloud-free observations to
 311 determine if the loss detections persist, the required number of HLS scenes depends on visibility of the target.
 312 Due to this, summarizing the DIST-ALERT in the DIST-ANN product will have some latency depending on
 313 the algorithmic calibration and detailed in subsequent documentation. Additional contextual layers are
 314 provided for disturbed pixels including: the date of initial disturbance, vegetation disturbance confidence,
 315 number of observed anomalies, and disturbance duration. An example of provisional versus confirmed alerts
 316 is shown in *Figure 11*.



317 Figure 10: Flow of processes and outputs of the DIST product suite.



318 Figure 11: Map showing a Quebec wildfire captured in the DIST-ALERT vegetation disturbance status from September
 319 13, 2023.

320 Output Product Layers

321 The layers detailed in **Tables 1** are output for each HLS scene/tile for which vegetation cover is estimated.
 322 For every HLS scene a per-pixel estimate of the current percent vegetation cover indicator and the current
 323 anomaly value are provided within the DIST-ALERT product. The anomaly value is defined as the
 324 difference in estimated percent vegetation cover between the seasonally normalized lower bound of historical
 325 vegetation cover (historic vegetation cover indicator) and the percent vegetation cover estimate from the
 326 current HLS scene. Only anomalies of vegetation loss are reported. Although disturbances must be reported
 327 for $\geq 50\%$ vegetation cover loss per the project requirements and validation activities, all disturbances with
 328 vegetation cover loss $\geq 10\%$ are tracked in the time-series. The maximum anomaly and duration layers can be
 329 leveraged to assess the magnitude and duration of disturbances. Given potential rapid vegetation recovery, the
 330 anomaly value corresponding to the date of maximum anomaly as well as the historical lower bound from
 331 that date are reported. As the historical lower bound corresponds to the date of maximum anomaly it is not
 332 reported for pixels without recorded anomalies. The vegetation cover estimate for the current year at the date

333 of maximum anomaly can be calculated from these two values. **Table 2** shows all the metadata of DIST-
 334 ALERT product, which can be found in the cmr.json metadata file in the package of DIST-ALERT product.

335 **Table 3** lists all the layers in the annual summary DIST-ANN product. And **Table 4** lists all the the metadata
 336 of DIST-ANN. The metadata file can be found in a cmr.json file of the DIST-ANN package. There will also
 337 be a comma delimited file(CSV) listing all the DIST-ALERT input files, HLS source files and image metadata.

338 Table 1: Product Raster Layers for DIST-ALERT

DIST-ALERT Raster Layer	Description	File name	Data type	Layer values
Vegetation disturbance status	Indication of vegetation cover loss (vegetation disturbance). The status label is based on the maximum anomaly value, confidence level, and whether it is ongoing or finished. “First” means the pixel has had an anomaly detection but no subsequent observations whether anomalous or not. “Provisional” means there have been two consecutive disturbance detections but not yet high confidence. “Confirmed” means that vegetation disturbance is detected with high confidence (≥ 400). The label “finished” is applied to confirmed disturbances that have had two consecutive no-anomaly observations or one 15 days or more after the last anomaly detection. If a new disturbance is detected, it will overwrite those in a “finished” state. These labels are reported for both above and below the 50% disturbance threshold based on the maximum anomaly value.	VEG - DIST - STAT US	UInt8	0: No disturbance 1: first <50% 2: provisional <50% 3: confirmed <50% 4: first $\geq 50\%$ 5: provisional $\geq 50\%$ 6: confirmed $\geq 50\%$ 7: confirmed <50%, finished 8: confirmed $\geq 50\%$, finished

369				255: No data	
370					
371	Current	The percent vegetation cover estimated for the current HLS scene for all land and water pixels.	VEG -IND	UInt 8	0-100:
372	vegetati				Estimated
373	on cover				percent
374	indicator				vegetatio
375					n
376				255: No data	
377					
378	Current	Difference between historical baseline and observed vegetation cover at the current date (vegetation loss of 0-100%). When >0, the sum of this anomaly value and the current vegetation cover indicator will be the historical vegetation cover estimate.	VEG - ANO M	UInt 8	0-100:
379	vegetati				Estimated
380	on				loss of
381	anomaly				percent
382	value				vegetatio
383		n			
384				255: No data	
385	Historic	Historical percent baseline value at the time of the maximum anomaly for disturbance pixels. A fill value is used for all non-disturbance pixels. Historical vegetation is calculated from all HLS scenes within a synchronous temporal window (± 15 days) from previous three calendar years to capture intra-annual/seasonal variation.	VEG - HIST	UInt 8	0-100:
386	al				Vegetatio
387	vegetati				n percent
388	on cover				200: No
389	indicator				disturban
390		ce			
391				255: No data	
392	Max	Difference between historical and current year observed vegetation cover at the date of maximum decrease (vegetation loss of 0-100%).. This layer can be used to threshold vegetation disturbance per a given sensitivity (e.g. disturbance of $\geq 20\%$ vegetation cover loss). The sum of the historical percent vegetation and the anomaly value will be the vegetation cover estimate for the current year.	VEG - ANO M- MAX	UInt 8	0-100:
393	vegetati				Maximu
394	on				m loss of
395	anomaly				percent
396	value				vegetatio
397		n			
398				255: No data	
399	Vegetati	Mean anomaly value since initial anomaly detection multiplied by the number of loss anomalies squared. Confidence is	VEG -	Int16	-1: No
400	on				data

392	Disturba	calculated until the anniversary date is reached, or a fixed number of consecutive non-anomalies are observed causing the status (VEG-DIST-STATUS) to change to “finished”.	DIST		0: No disturbance >0: Disturbance confidence
393	n		-		
394	Confide		CON		
395	n		F		
396	Layer				
397					
398					
399					
400	Date of initial vegetation disturbance	Day of first loss anomaly detection of the most recent disturbance event. Day denoted as the number of days since December 31, 2020.	VEG	Int16	-1: No data 0: No vegetation anomalies in the last year >0: Day of initial anomaly detection in the last year
401			-		
402			DIST		
403			-		
404			DAT		
405			E		
406					
407					
408	Number of detected vegetation loss anomalies	Total number of observations with anomalous low vegetation since initial anomaly detection (inclusive). Maximum of 254.	VEG	UInt8	0: No disturbance 1-254: Count of loss anomalies 255: No data
409			-		
410			COU NT		
411	Vegetation disturbance duration	Number of days of ongoing loss anomalies since initial anomaly detection (inclusive). Maximum duration is one year.	VEG	Int16	-1: No data 0: No disturbance 1-366: number
412			-		
413			DIST		
414			-		
415			DUR		
416					
417					

418
419
420
421
422
423
424
425
426
427
428
429
430
431
432
433
434
435
436
437
438
439
440
441
442
443
444
445
446
447
448
449
450
451
452
453
454
455
456

				of days from first anomaly to most recent anomaly detection
Date of last observation assessed for vegetation disturbance	Day of last quality assessed HLS observation flagged as land or water that also had sufficient observations for baseline calculation for vegetation disturbance algorithm. Day denoted as the number of days since December 31, 2020.	VEG - LAS T-DAT E	Int16	-1: No data ≥1: Last day assessed
Generic disturbance status	Indication of generic spectral difference. The status label is based on the maximum anomaly value, confidence level, and whether it is ongoing or finished. “First” means the pixel has had an anomaly detection but no subsequent observations whether anomalous or not. “Provisional” means there have been two consecutive disturbance detections but not yet high confidence. “Confirmed” means that disturbance is detected with high confidence. The label “finished” is applied to confirmed disturbances that have had two consecutive no-anomaly observations or one 15 days or more after the last anomaly detection. If a new disturbance is detected, it will overwrite those in a “finished” state. These labels are reported for both above a low and high threshold based on the maximum spectral anomaly.	GEN - DIST - STAT US	UInt8	0: No disturbance 1: first low 2: provisional low 3: confirmed low 4: first high 5: provisional high 6: confirmed high 7: confirmed low, finished

457
458
459
460
461
462
463
464
465
466
467
468
469
470
471
472
473
474
475
476
477
478
479
480
481
482
483
484

				8: confir med high, finished 255: No data
Current generic disturba nce anomaly value	Spectral distance between current HLS scene reflectance and the reflectance of the previous three calendar years within ± 15 calendar days. Calculated by Mahalanobis distance.	GEN - ANO M	Int16	-1: No data 0: No disturban ce >0: Spectral distance
Generic disturba nce maximu m anomaly value	Maximum spectral distance between a current year HLS scene reflectance and the composite reflectance of previous calendar years.	GEN - ANO M- MAX	Int16	-1: No data 0: No disturban ce >0: Spectral distance
Generic Disturba nce Confide nce Layer	Mean spectral distance since initial spectral anomaly detection times the number of spectral anomalies above a threshold, until the anniversary date is reached, or a fixed number of consecutive non-anomalies are observed.	GEN - DIST - CON F	Int16	-1: No data 0: No disturban ce >0: Disturban ce confidenc e
Date of initial generic disturba nce	Day of first spectral anomaly detection of the most recent disturbance event. Day denoted as the number of days since December 31, 2020.	GEN - DIST - DAT E	Int16	-1: No data 0: No spectral anomalie s in the last year

485
486
487
488
489
490
491
492
493
494
495
496
497
498
499
500
501
502
503
504
505
506
507
508
509
510
511
512

				>0: Day of initial anomaly detection in the last year
Number of detected spectral anomalies	Total number of observations with spectral reflectance anomalies (inclusive). Maximum of 254.	GEN - DIST - COUNT	UInt8	0: No disturbance 1-254: Count of loss anomalies 255: No data
Generic disturbance duration	Number of days of ongoing spectral reflectance anomalies since initial anomaly detection (inclusive). Maximum duration is one year.	GEN - DIST - DUR	Int16	-1: No data 0: No disturbance 1-366: number of days from first anomaly to most recent anomaly detection
Date of last observation assessed for generic disturbance	Day of last quality assessed HLS observation flagged as land that also had sufficient observations for baseline calculation for generic disturbance algorithm. Day denoted as the number of days since December 31, 2020.	GEN - LAST-DATE	Int16	-1: No data ≥1: Last day assessed

513	Data mask	Mask of pixels the algorithms are applied to in the current HLS scene. Based on the Fmask layer of the source HLS granule.	DAT A- MAS K	UInt 8	0: Not land 1: Land
514					

515 Table 2: DIST-ALERT metadata

516	Attribute	Description
517	GranuleUR	The granule ID for each DIST-ALERT. Format: OPERA_L3_DIST-ALERT-HLS_Tile_YYYYMMDDTHHMMSSZ_YYYYMMDDTHHMMSSZ_S2A_30_v1
518		
519		
520	TemporalExtent: RangeDateTime	The DIST-ALERT product versionTemporal extent of the HLS data, flagged as BeginningDateTime and EndingDateTime. Format: YYYY-MM-DDTHH:MM:SS.SSSSSSZ
521	ProviderDates	The date of DIST-ALERT product be provided
522	CollectionReferen ce:ShortName	The short name of the collection, OPERA_L3_DSIT-ALERT-HLS_V1
523	CollectionReferen ce:Version	The DIST-ALERT product version
524	DataGranule: DayNightFlag	Flag if the image is during the day or night
525	DataGranule: ProductionDateTi me	DIST-ALERT product processing date. Format: YYYY-MM-DDTHH:MM:SS.SSSSSSZ
526	Platforms	Name of the sensor platform (e.g. Landsat-8/9 or Sentinel-2 A/B)
527	Instruments	Name of the sensor instrument (e.g. OLI or MSI)
528	SpatialExtent	The longitude and latitude boundary of the image
529	CloudCover	The percentage of cloud and cloud shadow in the DIST-ALERT product (copied from HLS)
530	Input_DIST- ALERT_granule	The input DIST-ALERT granule ID

531	BaselineCalendarWindow	Number of days before and after the calendar date used to create the baseline
532	BaselineYearWindow	Number of previous years used to create the baseline
533	BaselineImageIds	List of the input HLS granules used to create the baseline
534	ValidationLevel	The validation level of the product
535	HLSGranuleUR	Name of the input HLS granule used to generate the DIST-ALERT product
536	SENSOR_PROD UCT_ID	The source Landsat or Sentinel-2 data ID
537	SPATIAL_COVE RAGE	The area percentage of the tile with data (copied from HLS)
538	MGRS_TILE_ID	The tile ID
539	HLS_PROCESSI NG_TIME	The input HLS granule processing date. Format: YYYY-MM-DDTHH:MM:SS.SSSSSSZ.
541	SENSING_TIME	The sensing time provided with the source Landsat or Sentinel-2 image. Format: YYYY-MM-DDTHH:MM:SSZ.
542	HORIZONTAL_ CS_CODE	The code for the coordinate system, eg: "EPSG:32655"
543	HORIZONTAL_ CS_NAME	The name of the coordinate system, eg: "UTM, WGS84, UTM ZONE 55"
544	ULX	The E-W coordinate of the upper left within the given coordinate system
545	ULY	The N-S coordinate of the upper left within the given coordinate system

546 Table 3: Product Raster Layers for DIST-ANN

547	DIST-ANN Raster Layer	Description	File name	Data type	Layer values
548	Vegetation disturbance status	Status corresponding to the highest confidence	VEG- DIST- STAT US	UInt 8	0: No disturbance 3: confirmed <50% ongoing
549		vegetation disturbance confirmed within the year.			
550		Status classes identify confirmed ongoing			
551		disturbance, confirmed finished disturbance, and			

552		confirmed disturbance initially detected in previous			6: confirmed
553		year for both <50% and ≥50%, and no disturbance.			≥50% ongoing
554					7: confirmed
555					<50% finished
556					8: confirmed
557					≥50% finished
558					9: confirmed
559					previous year
560					<50%
561					10: confirmed
562					previous year
563					≥50%
564					255: No data
565	Historical vegetation cover indicator	Historical percent vegetation from composite of HLS scenes during the same time period of the maximum anomaly for disturbance pixels. A fill value is used for all non-disturbance pixels. Historical vegetation is calculated from a synchronous temporal window from previous calendar years to capture intra-annual/seasonal variation.	VEG- HIST	UInt 8	0-100: Vegetation percent 200: No disturbance 255: No data
566	Maximum vegetation cover indicator	For non-disturbance pixels, maximum annual vegetation fraction from the HLS time-series data will be reported. For disturbance pixels, the vegetation fraction from the date of maximum anomaly will be reported.	VEG- IND- MAX	UInt 8	0-100: Estimated loss of percent vegetation 255: No data
567	Maximum vegetation anomaly value	Difference between historical vegetation cover and vegetation cover at the date of maximum decrease (vegetation loss of 0-100%). This layer can be used to threshold vegetation disturbance per a given sensitivity (e.g. disturbance of ≥20% vegetation cover loss).	VEG- ANO M- MAX	UInt 8	0-100: Maximum loss of percent vegetation 255: No data
568					
569	Vegetation Disturbance Confidence Layer	Mean anomaly value since initial anomaly detection times the number of loss anomalies squared, until the anniversary date is reached, or a fixed number of consecutive non-anomalies are observed.	VEG- DIST- CONF	Int16	-1: No data 0: No disturbance >0: Disturbance confidence
570					
571					

572	573	Date of initial vegetation disturbance	Day of first loss anomaly. Day denoted as the number of days since December 31, 2020.	VEG-DIST-DATE	Int16	-1: No data 0: No disturbance >0: Day of first loss anomaly detection					
574	575	Number of detected vegetation loss anomalies	Total number of loss anomalies since initial anomaly detection(inclusive). Maximum of 254.	VEG-DIST-COUNT	UInt8	0: No disturbance 1-254: Count of loss anomalies 255: No data					
576	577	578	579	580	581	582	Vegetation disturbance duration	Number of days of ongoing loss anomalies since initial anomaly detection (inclusive). Maximum duration is one year.	VEG-DIST-DUR	Int16	-1: No data 0-366: number of days from first anomaly to most recent anomaly detection
583	584	Indicator of vegetation disturbance from previous year	Indicator of whether the highest confidence vegetation disturbance event confirmed within the year (corresponding to the above layers) was initially detected in the previous calendar year.	VEG-CONF-PREV	UInt8	0: no disturbance 1: confirmed low previous year, 2: confirmed high previous year, 255: no data					
585	586	Count of confirmed vegetation disturbance events	Count of distinct confirmed vegetation disturbance events.	VEG-CONF-COUNT	UInt8	≥0: count of confirmed vegetation disturbance events 255: no data					
587	588	589	590	Minimum three year vegetation	The minimum vegetation cover of the current year and two previous years with stricter aerosol filtering. Becomes input to the following year's DIST-ALERT product.	VEG-IND-3YR-MIN	UInt8	0-100: Vegetation percent 255: No data			

591	cover				
592	indicator				
593	Date of last observation assessed for vegetation disturbance	Day of last quality assessed HLS observation flagged as land that also had sufficient observations for baseline calculation for vegetation disturbance algorithm. Day denoted as the number of days since December 31, 2020.	VEG-LAST-DATE	Int16	-1: No data 0: Never flagged as land >0: Day of last land observation
594	Generic disturbance status	Status corresponding to the highest confidence generic spectral difference confirmed within the year. Status classes identify confirmed ongoing disturbance, confirmed finished disturbance, and confirmed disturbance initially detected in previous year for both above a low and high threshold and no disturbance.	GEN-DIST-STAT US	UInt8	0: No disturbance 3: confirmed low, ongoing 6: confirmed high, ongoing 7: confirmed low, finished 8: confirmed high, finished 9: confirmed low, previous year 10: confirmed high, previous year 255: No data
595					
596					
597					
598					
599					
600					
601					
602					
603					
604					
605					
606					
607	Generic maximum disturbance anomaly value	Maximum spectral distance between a current year HLS scene reflectance and the composite reflectance of previous calendar years.	GEN-ANOM-MAX	Int16	-1: No data 0: No disturbance >0: Spectral distance
608	Generic Disturbance Confidence Layer	Mean spectral distance since initial spectral anomaly detection times the number of spectral anomalies above a threshold, until the anniversary date is reached, or a fixed number of consecutive non-anomalies are observed.	GEN-DIST-CONF	Int16	-1: No data 0: No disturbance >0: Disturbance confidence
609					
610	Date of generic	Day of first spectral anomaly. Day denoted as the number of days since December 31, 2020.	GEN-DIST-	Int16	-1: No data
611					

612	initial		DATE		0: No
613	disturbance				disturbance
614	anomaly				>0: Day of first
615					anomaly
616					detection
617	Number of	Total number of observations with a spectral anomaly	GEN-	UInt	0: No loss
618	detected	since initial anomaly detection (inclusive). Maximum	DIST-	8	anomalies
619	spectral	of 254.	COUN-		1-254: Count
	anomalies		T		of loss
					anomalies
					255: No data
620	Generic	Number of days of ongoing spectral anomalies since	GEN-	Int16	-1: No data
621	disturbance	initial anomaly detection (inclusive). Maximum	DIST-		0-366: number
622	duration	duration is one year.	DUR		of days from
623					first anomaly
624					to most recent
625					anomaly
626					detection
627	Indicator of	Indicator of whether the highest confidence generic	GEN-	UInt	0: no
628	generic	disturbance event confirmed within the year	CONF	8	disturbance
	disturbance	(corresponding to the above GEN layers) was	-PREV		1: confirmed
	from	initially detected in the previous calendar year.			low previous
	previous				year,
	year				2: confirmed
629					high previous
					year,
					255: no data
630	Count of	Count of distinct confirmed generic disturbance	GEN-	UInt	>0: count of
	confirmed	events.	CONF	8	confirmed
	generic		-		generic
	disturbance		COUN-		disturbance
	events		T		alert
					255: no data
631	Date of last	Day of last quality assessed HLS observation flagged	GEN-	Int16	-1: No data
632	observation	as land that also had sufficient observations for	LAST-		0: Never
633	assessed for	baseline calculation for generic disturbance	DATE		flagged as land
634	generic	algorithm. Day denoted as the number of days since			
635	disturbance	December 31, 2020.			

636
637
638

639

640
641
642
643
644
645
646
647
648
649
650
651
652
653
654
655
656

>0: Day of last
land
observation

Table 4: DIST-ANN Metadata

Attribute	Description
GranuleUR	The granule ID for each DIST-ANN. Format: OPERA_L3_DIST-ANN-HLS_Tile_YYYY_YYYYMMDDTHHMMSSZ_30_v1
TemporalExtent: RangeDateTime	Temporal extent of the HLS data of the input year, flagged as BeginningDateTime and EndingDateTime. Format: YYYY-MM-DDTHH:MM:SS.SSSSSSZ
ProviderDates	The date-time of when the granule was sent to LP-DAAC. Format: YYYY-MM-DDTHH:MM:SS.SSSSSSZ
CollectionReference:ShortName	OPERA_L3_DIST-ANN-HLS_V1
CollectionReference:Version	The DIST-ANN product version
SpatialExtent	The longitude and latitude boundary of the image
CloudCover	The percentage of no-data in the DIST-ANN product
Platforms	Names of the input sensor platforms (e.g. Landsat 8/9 and Sentinel-2 A/B)
Instruments	Names of the input sensor instruments (e.g. OLI and Sentinel-2 MSI)
ValidationLevel	The validation level of the product
SPATIAL_COVERAGE	The area percentage of the tile with data
MGRS_TILE_ID	The tile ID
HORIZONTAL_CS_CODE	The code for the coordinate system, eg: "EPSG:32655"
HORIZONTAL_CS_NAME	The name of the coordinate system, eg: "UTM, WGS84, UTM ZONE 55"
ULX	The E-W coordinate of the upper left within the given coordinate system

657	ULY	The N-S coordinate of the upper left within the given coordinate system
658	PROCESSING_D ATETIME	DIST-ANN product processing date. Format: YYYY-MM-DDTHH:MM:SSZ.

659 3.2.1. Mathematical Theory Assumptions

660 As with any machine learning algorithm, its performance is only as good as its input data sets. High
 661 resolution drone images are collected as the training data for vegetation fraction estimation. We have iterated
 662 to collect the representative land cover and land use to fill different compositions in the principle components
 663 space and to cover all ranges of vegetation cover.

664 3.3. Algorithm Input Variables

665 Variable #1

666 **NAME** **HLS FMASK**
 667 **LONG NAME** **HLS quality assessment layer**
 668 **UNIT** **Unit8**

669 Variable #2

670 **NAME** **HLS RED**
 671 **LONG NAME** **HLS red band**
 672 **UNIT** **Int16**

673 Variable #3

674 **NAME** **HLS NIR**
 675 **LONG NAME** **HLS near infrared band**
 676 **UNIT** **Int16**

677 Variable #4

678 **NAME** **HLS SWIR1**
 679 **LONG NAME** **HLS shortwave infrared band 1**
 680 **UNIT** **Int16**

681 Variable #5

682 **NAME** **HLS SWIR2**
683 **LONG NAME** **HLS shortwave infrared band 2**
684 **UNIT** **Int16**

685 **Variable #6**

686 **NAME** **Ocean mask**
687 **LONG NAME** **Global ocean mask**
688 **UNIT** **Unit8**

689 **3.4. Algorithm Output Variables**

690 **Variable #1**

691 **NAME** **VEG-DIST-TATUS**
692 **LONG NAME** **Vegetation disturbance status**
693 **UNIT** **UInt8**

694 **Variable #2**

695 **NAME** **VEG-HIST**
696 **LONG NAME** **Historical vegetation cover indicator**
697 **UNIT** **UInt8**

698 **Variable #3**

699 **NAME** **VEG-IND-MAX**
700 **LONG NAME** **Maximum vegetation cover indicator**
701 **UNIT** **UInt8**

702 **Variable #4**

703 **NAME** **VEG-ANOM-MAX**
704 **LONG NAME** **Maximum vegetation anomaly value**
705 **UNIT** **UInt8**

706 **Variable #5**

707 **NAME** **VEG-DIST-CONF**
708 **LONG NAME** **Vegetation Disturbance Confidence Layer**
709 **UNIT** **Int16**

710 **Variable #6**

711 **NAME** **VEG-DIST-DATE**
712 **LONG NAME** **Date of initial vegetation disturbance**
713 **UNIT** **Int16**

714 **Variable #7**

715 **NAME** **VEG-DIST-COUNT**
716 **LONG NAME** **Number of detected vegetation anomalies**
717 **UNIT** **UInt8**

718 **Variable #8**

719 **NAME** **VEG-DIST-DUR**
720 **LONG NAME** **Vegetation disturbance duration**
721 **UNIT** **Int16**

722 **Variable #9**

723 **NAME** **VEG-LAST-DATE**
724 **LONG NAME** **Date of last observation assessed for vegetation disturbance**
725 **UNIT** **Int16**

726 **Variable #10**

727 **NAME** **GEN-DIST-STATUS**
728 **LONG NAME** **Generic disturbance status**
729 **UNIT** **UInt8**

730 **Variable #11**

731 **NAME** **GEN-ANOM-MAX**
732 **LONG NAME** **Generic maximum disturbance anomaly value**
733 **UNIT** **Int16**

734 **Variable #12**

735 **NAME** **GEN-DIST-CONF**
736 **LONG NAME** **Generic Disturbance Confidence Layer**
737 **UNIT** **Int16**

738 **Variable #13**

739 **NAME** GEN-DIST-COUNT
740 **LONG NAME** Number of detected spectral anomalies
741 **UNIT** UInt8

742 **Variable #14**

743 **NAME** GEN-DIST-DUR
744 **LONG NAME** Generic disturbance duration
745 **UNIT** Int16Int16

746 **Variable #15**

747 **NAME** GEN-LAST-DATE
748 **LONG NAME** Date of last observation assessed for generic disturbance
749 **UNIT** Int16

750 **Variable #16**

751 **NAME** VEG-IND
752 **LONG NAME** Current vegetation cover indicator
753 **UNIT** UInt8

754 **Variable #17**

755 **NAME** VEG-ANOM
756 **LONG NAME** Current vegetation anomaly value
757 **UNIT** UInt8

758 **Variable #18**

759 **NAME** GEN-ANOM
760 **LONG NAME** Current generic disturbance anomaly value
761 **UNIT** Int16

762 **Variable #19**

763 **NAME** GEN-DIST-DATE
764 **LONG NAME** Date of initial generic disturbance
765 **UNIT** Int16

766 **Variable #20**

767 **NAME** LAND-MASK

768 **LONG NAME** Land mask

769 **UNIT** UInt8

770 **Variable #21**

771 **NAME** VEG-CONF-PREV

772 **LONG NAME** Indicator of vegetation disturbance from previous year

773 **UNIT** UInt8

774 **Variable #22**

775 **NAME** VEG-CONF-COUNT

776 **LONG NAME** Count of confirmed vegetation disturbance events

777 **UNIT** UInt8

778 **Variable #23**

779 **NAME** VEG-IND-3YR-MIN

780 **LONG NAME** Minimum three year vegetation cover indicator

781 **UNIT** UInt8

782 **Variable #24**

783 **NAME** GEN-CONF-PREV

784 **LONG NAME** Indicator of generic disturbance from previous year

785 **UNIT** UInt8

786 **Variable #25**

787 **NAME** GEN-CONF-COUNT

788 **LONG NAME** Count of confirmed generic disturbance events

789 **UNIT** UInt8

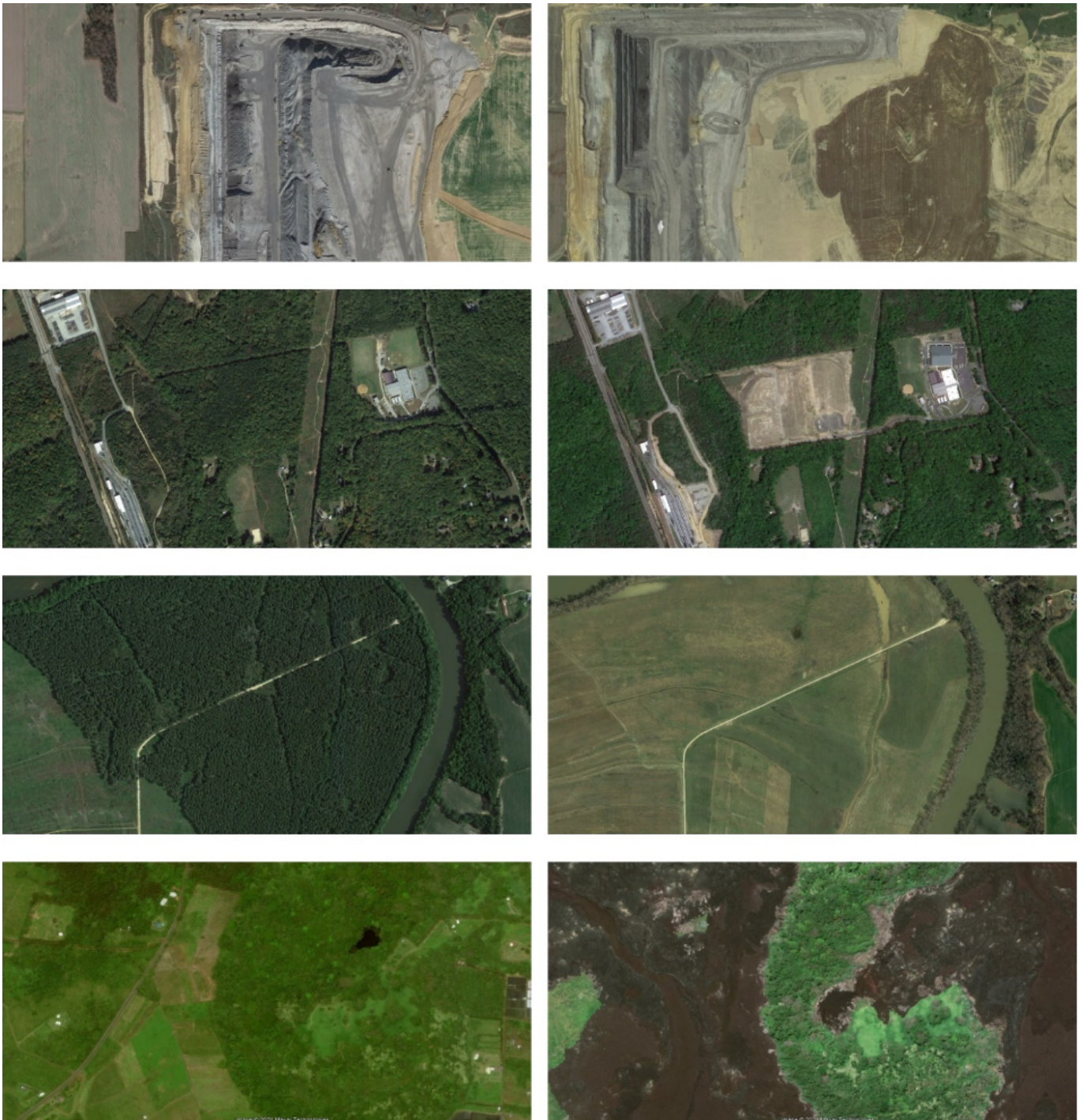
790 **4. Algorithm Usage Constraints**

791 The principal limitation to the DIST products is there is no attribution of the causes of disturbances and the
792 type is only defined as vegetation loss or general. The vegetation algorithm is a generic indicator of
793 vegetation loss, whether due to logging, landslides, development or any other event resulting in reduced
794 vegetation cover. Example vegetation loss dynamics to be detected with the DIST products are shown in
795 **Figure 12**, with a resulting need for users to place appropriate context on the outputs. The dynamics detected
796 with the spectral distance algorithm are spread across an even further range including both vegetation loss
797 and gain and change in non-vegetated surfaces, such as a parking lot replaced with a building or a lava flow
798 in the desert. Future iterations of the algorithm may include reference cover state or supplementary algorithms
799 to assign dynamics of antecedent land cover or land use, change factor, and resulting cover.

800 Additionally, some land disturbances will not be detected by the vegetation disturbance layer, including
801 vegetation recovery, phenological and intra-annual vegetation changes, urban development within urban
802 sprawl (e.g. buildings being replaced or being demolished) or more generally, any urban changes of non-
803 vegetated areas (e.g. a highway being built over a desert landscape), lava flows over a rocky, non-vegetated
804 terrain. However, some of these will be able to be detected with the spectral distance algorithm, but areas
805 with more spectral variation in the baseline will be less likely to detect changes. Land use dynamics that are
806 part of an annual practice, for example crop rotations or tilling practices, or fire as maintenance of vegetative
807 cover, for example savanna fires in tropical Africa, will not be flagged as disturbance if they occur within the
808 same temporal window (± 15 days) in the previous three years. Such changes are part of a regular and
809 repeated interannual land use, and as such within normal near-term variability in vegetative cover. That said,
810 very often these regular land changes may be shifted by more than 15 days between years and then they will
811 appear within DIST-ALERT.

812 The algorithms of DIST-ALERT require accurate detection of land observations uncontaminated by cloud,
813 haze, shadow, or snow/ice. If contaminated pixels pass through to the disturbance algorithms then these
814 masking errors propagate through the product. For example, when pixels with cloud cover are not masked
815 out, the vegetation fraction model will be applied to that pixel and result in a low vegetation cover estimate. If
816 these pixels are over a vegetated area then they will be marked as vegetation loss. Tracking these pixels
817 through subsequent observations can mitigate these commission errors as cloud omission errors are not likely
818 to regularly repeat over the same pixels, in which case they would be removed from the status layers. Cloud
819 commission errors can also propagate omission errors in DIST-ALERT. Some bright targets such as the white
820 roofs of buildings, are regularly flagged as cloud and these pixels then never pass through to the DIST-
821 ALERT disturbance algorithms. For now, the product is relying on the identification of cloud, shadow, and
822 snow/ice provided within the Fmask layer of the HLS input.

823 Although measuring vegetation cover is beyond the scope of the DIST product, the auxiliary vegetation
824 cover indicator layers that are used by the internal models for identifying areas of disturbance can be used for
825 additional correlative analysis directly. For example, the maximum vegetation anomaly can be harnessed to
826 threshold vegetation cover loss at a higher sensitivity (i.e., loss smaller than 50%) and the current vegetation
827 cover indicator can be tracked over time to evaluate possible recovery trends. Constraints on the use of the
828 vegetation cover indicator will be determined via validation efforts and result in guidance to users in applying
829 the time-series vegetation cover estimates.



830 Figure 12: Example dynamics that will be detected by the DIST algorithm: from top to bottom, open pit coal mining in
831 southwest Indiana (centered at 87.308W, 39.026N), commercial land use expansion in northern Virginia (77.433W,
832 38.215N), conversion of secondary forest to cropland in northern Alabama (85.796W, 34.124N), and loss of vegetation
833 due to lava flow on Hawaii (154.842W, 19.500N). Imagery from GoogleEarth.

834 5. Performance Assessment

835 5.1. Validation Methods

836 Validation of DIST product will have two important categories of activities:

- 837 1. Validation of the disturbance detection layers in the DIST-ALERT and DIST-ANN products using high-
838 resolution derived disturbance data.
- 839 2. Assessment activities related to the current vegetation cover indicator within the DIST-ALERT product.

840 The first category will be used to determine the accuracy of the vegetation disturbance. The second category
841 is related to reporting the statistical relationship of the intermediate vegetation cover indicator layer used by
842 the disturbance algorithm and in-situ vegetation cover as determined by field work.

843 To validate both the DIST-ALERT and the DIST-ANN we will employ a stratified random sample of
844 reference data in a manner similar to that of the study of (Ying et al., 2017). The global population of all 30m
845 pixels aligned with the HLS pixel grid will be stratified based on disturbance presence and an equal area
846 sample of 30m pixels will be selected. For each pixel randomly selected as a validation site, 3m PlanetScope
847 data will be employed to create reference data of disturbance status (**Figure 13**) and the initial date of
848 disturbance events, where feasible. This reference data will then be compared to the selected pixel in the
849 DIST-ALERT time-series and the DIST-ANN product to ensure the requirement is met. The reference data
850 for each validation site are created by mapping or visually interpreting 30m HLS pixel footprints from time-
851 series high-resolution PlanetScope data. An analyst marks all time steps of the high-resolution data that have a
852 $\geq 50\%$ loss of vegetation cover, resulting in a yes/no reference time-series of $\geq 50\%$ vegetation cover loss. The
853 analyst will also mark the initial date of any discernible loss events $< 50\%$ or whether there was no
854 disturbance.

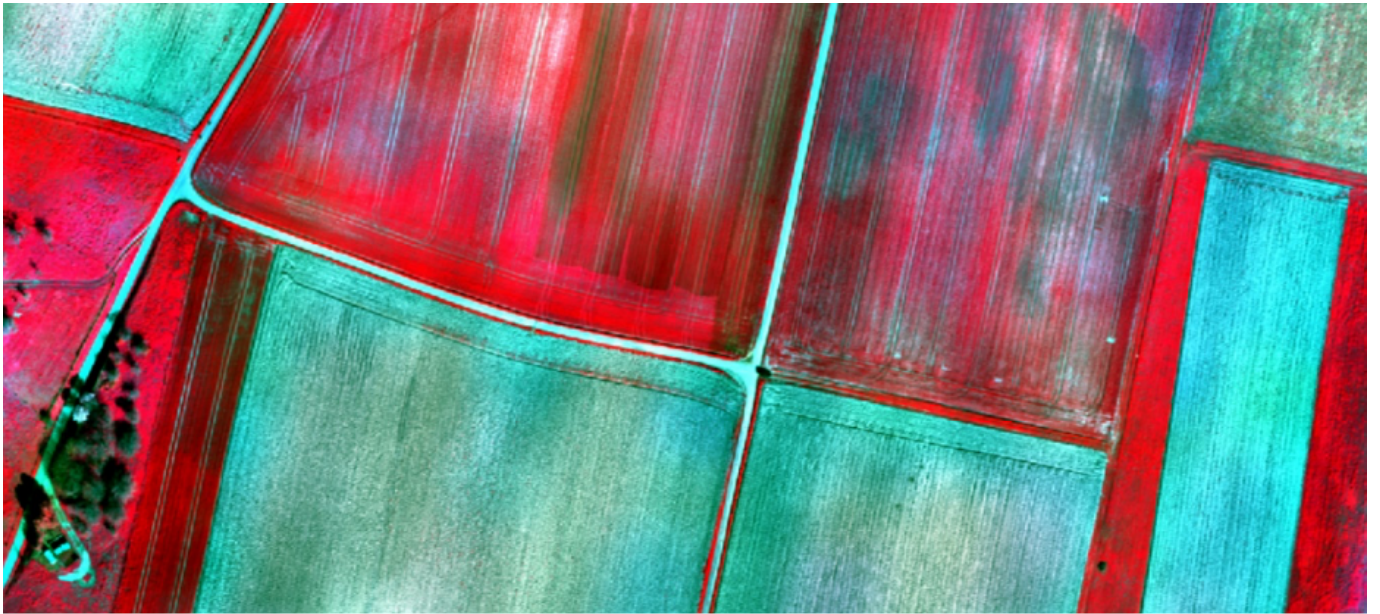
855 For vegetation disturbance validation, per the requirements, the vegetation disturbances with anomalies $\geq 50\%$
856 mapped in the DIST-ALERT will be considered disturbed and all other land observations will be considered
857 no-disturbance. As the DIST-ALERT product is released at the cadence of the HLS input dataset, the
858 accuracy of the DIST-ALERT product is calculated from all HLS time-steps with respect to the reference
859 disturbance time-series so that the reported accuracy will apply to all observations and thus all phenological
860 stages. The DIST-ALERT product will be compared to the reference time-series by matching the respective
861 dates. There is an associated date for each disturbance/no-disturbance label in the reference time-series which
862 corresponds to the time of the high-resolution Planet acquisitions. For each HLS acquisition date, DIST-
863 ALERT will be compared with the reference data label from the same date when possible. For HLS dates
864 without a coincident reference label, if the closest preceding and following reference date have the same
865 label, this is compared with the DIST-ALERT label. If the two reference dates have different labels this time
866 step is excluded as it is unknown when the disturbance occurred between these two dates. Given that the
867 validation assessment covers an entire year with all HLS acquisition dates evaluated, all seasons are assessed
868 and any errors due to intra-annual variation will be quantified.



869 Figure 13: Example validation data from ~3-4m PlanetScope imagery over a residential expansion site near Dallas,
870 Texas, centered at 32.654N,97.500W. From left to right, image from 12-31-2019, image from 12-29-2020, and mapped
871 vegetation loss in black overlay. All cloud-free PlanetScope data (not shown here) will be used to refine data of
872 disturbance estimation. Sample 30m HLS pixel shown in red outline exhibits vegetation loss.

873 The DIST-ALERT has two types of disturbances: provisional and confirmed. Both types of disturbances in
874 DIST-ALERT will be evaluated against the high-resolution derived time-series. Typically, the confirmed
875 disturbances in the DIST-ALERT product are expected to have a higher accuracy as they have been
876 repeatedly observed. However, given that for minimum latency DIST-ALERT products may be used as soon
877 as HLS scenes are characterized and before a new disturbance can be confirmed from repeat observations,
878 we will also validate provisional alerts. The overall user's and producer's accuracies of both products will be
879 reported and provide a globally representative measure of DIST product performance.

880 The assessment of the vegetation cover indicator layer pertains to the vegetation layers of the DIST suite used
881 as inputs to the disturbance detection algorithms and distributed with the DIST product. Although this layer is
882 without a formal requirement, providing a general assessment of this intermediate layer's utility is valuable for
883 users and for increasing the transparency of the disturbance detection algorithm. The assessment uses 3 by 3
884 pixel grids of vegetation cover derived from field data collected contemporaneously with a Landsat 8 or
885 Sentinel 2 overpass. Each grid is aligned with the DIST-ALERT product pixels and is produced using sub-
886 meter maps from field data collected using a drone-based multi-spectral sensor, with example data shown in
887 **Figure 14**. The field data are associated with a given date and compared to the DIST-ALERT from the same
888 day as the field work. Specifically, the vegetation indicator layer is compared to the co-located 3 by 3 grid of
889 vegetation cover derived from the field work collected during different seasons. A comparison of the
890 vegetation indicator layer with respect to field reference maps will be reported, including RMSE and R^2 .



891 Figure 14: Example 4cm NIR-RED-GREEN imagery over an agricultural landscape using a WingtraONE Gen II drone
892 with a Mica-Sense Red Edge-MX multi-spectral camera. Each sample site will be characterized into yes/no vegetation cover,
893 for both photosynthetically active and photosynthetically and non-photosynthetically active data.

894 5.2. Uncertainties

895 Confusion matrices of yes/no disturbance accuracies and associated uncertainties will be calculated from the
896 global sample of reference data as compared to instantaneous DIST-ALERT and annual summary DIST-
897 ANN data similar to the method outlined by (Ying et al., 2017). Overall accuracy for the disturbances $\geq 50\%$
898 of DIST-ALERT is specified to exceed 80% and of DIST-ANN, 90% and both have an overall accuracy of
899 99%. For vegetation cover, we will report correlation measures for our opportunistically acquired drone-
900 based field data.

901 5.3. Validation Errors

902 Errors will be assessed and assigned to categories. Errors of omission, for example disturbances unrelated to
903 vegetation loss, will be quantified and their overall contribution to error calculated, justifying or not the use of
904 a complementary/back-up spectral distance algorithm. Both omission and commission errors will be
905 aggregated by climate domain/ecozone and disturbance type. In this way, users will know which
906 applications may be more readily supported by the DIST products.

907 6. Algorithm Implementation

908 6.1. Algorithm Availability

909 github.com/gladumd/OPERA_DIST/

910 The implementation codes of the algorithm are open to the public on GitHub.

911 **6.2. Input Data Access**

912 <https://search.earthdata.nasa.gov/search?q=HLS>

913 The DIST product employs single-date HLS tiles, each processed for all valid land observations. HLS data
914 access is through the Land Processes Distributed Active Archive Center (LPDAAC). Daily input volumes
915 range from 0.5-2.0Tb and processed outputs are estimated to be 0.5Tb daily.

916 **6.3. Output Data Access**

917 <https://search.earthdata.nasa.gov/search?q=OPERA%20HLS%20alert>

918 Final product layers are available through the LPDAAC. Users can access the data product through NASA's
919 Earthdata Search.

920 **7. Contact Details**

921 Matthew , Hansen

922 URL: <https://glad.umd.edu/team/matthew-hansen>

923 Contact mechanism: Email: mhansen@umd.edu

924 Role(s) related to this ATBD: Supervision, Writing – original draft, Writing – review & editing

925 Affiliation: University of Maryland, Department of Geographical Sciences, Global Land Analysis and
926 Discovery (GLAD) laboratory

927 Amy , Pickens

928 URL: <https://glad.umd.edu/team/amy-hudson-pickens>

929 Contact mechanism: Email: ahudson2@umd.edu

930 Role(s) related to this ATBD: Writing – original draft, Writing – review & editing, Corresponding Author

931 Affiliation: University of Maryland, Department of Geographical Sciences, Global Land Analysis and
932 Discovery (GLAD) laboratory

933 Zhen, Song

934 URL: <https://glad.umd.edu/team/zhen-song>

935 Contact mechanism: Email: zhensong@umd.edu

936 Role(s) related to this ATBD: Writing – review & editing, Validation

937 Affiliation: University of Maryland, Department of Geographical Sciences, Global Land Analysis and
938 Discovery (GLAD) laboratory

8. References

- 939
- 940 Adams, J.,B., Sabol, D.,E., Kapos, V., Almeida Filho, R., Roberts, D.,A., Smith, M.,O. & Gillespie, A.,R.
- 941 (1995). Classification of multispectral images based on fractions of endmembers: Application to land-cover
- 942 change in the Brazilian Amazon. *Remote sensing of Environment*, 52(2), 137--154.
- 943 Carroll, M., Townshend, J., Hansen, M., DiMiceli, C., Sohlberg, R. & Wurster, K. (2010). MODIS
- 944 vegetative cover conversion and vegetation continuous fields. 725--745.
- 945 Claverie, M., Ju, J., Masek, J.,G., Dungan, J.,L., Vermote, E.,F., Roger, J., Skakun, S.,V. et al. (2018). The
- 946 Harmonized Landsat and Sentinel-2 surface reflectance data set. *Remote sensing of environment*, 219, 145-
- 947 -161.
- 948 Davies, D.,K., Ilavajhala, S., Wong, M.,M. & Justice, C.,O. (2008). Fire information for resource
- 949 management system: archiving and distributing MODIS active fire data. *IEEE Transactions on Geoscience*
- 950 *and Remote Sensing*, 47(1), 72--79.
- 951 DeFries, R., Hansen, M., Steininger, M., Dubayah, R., Sohlberg, R. & Townshend, J. (1997). Subpixel
- 952 forest cover in central Africa from multisensor, multitemporal data. *Remote Sensing of Environment*, 60(3),
- 953 228--246.
- 954 Foley, J.,A., DeFries, R., Asner, G.,P., Barford, C., Bonan, G., Carpenter, S.,R., Chapin, F.,S. et al. (2005).
- 955 Global Consequences of Land Use. *Science*, 309(5734), 570--574.
- 956 Gitelson, A.,A., Kaufman, Y.,J., Stark, R. & Rundquist, D. (2002). Novel algorithms for remote estimation of
- 957 vegetation fraction. *Remote Sensing of Environment*, 80(1), 76--87. [https://doi.org/10.1016/S0034-](https://doi.org/10.1016/S0034-4257(01)00289-9)
- 958 [4257\(01\)00289-9](https://doi.org/10.1016/S0034-4257(01)00289-9)
- 959 Hansen, M., DeFries, R., Townshend, J., Carroll, M., Dimiceli, C. & Sohlberg, R. (2003). Global percent
- 960 tree cover at a spatial resolution of 500 meters: First results of the MODIS vegetation continuous fields
- 961 algorithm. *Earth Interactions*, 7(10), 1--15.
- 962 Hansen, M., DeFries, R., Townshend, J., Sohlberg, R., Dimiceli, C. & Carroll, M. (2002). Towards an
- 963 operational MODIS continuous field of percent tree cover algorithm: examples using AVHRR and MODIS

- 964 data. *Remote Sensing of Environment*, 83(1-2), 303--319.
- 965 Hansen, M., Egorov, A., Potapov, P., Stehman, S., Tyukavina, A., Turubanova, S., Roy, D.,P. et al. (2014).
966 Monitoring conterminous United States (CONUS) land cover change with web-enabled Landsat data
967 (WELD). *Remote sensing of Environment*, 140, 466--484.
- 968 Hansen, M.,C., Krylov, A., Tyukavina, A., Potapov, P.,V., Turubanova, S., Zutta, B., Ifo, S. et al. (2016).
969 Humid tropical forest disturbance alerts using Landsat data. *Environmental Research Letters*, 11(3), 034008.
- 970 Hansen, M.,C., Potapov, P.,V., Moore, R., Hancher, M., Turubanova, S.,A., Tyukavina, A., Thau, D. et al.
971 (2013). High-resolution global maps of 21st-century forest cover change. *Science*, 342(6160), 850--853.
- 972 Jiang, Z., Huete, A.,R., Chen, J., Chen, Y., Li, J., Yan, G. & Zhang, X. (2006). Analysis of NDVI and scaled
973 difference vegetation index retrievals of vegetation fraction. *Remote Sensing of Environment*, 101(3), 366-
974 -378. <https://doi.org/10.1016/j.rse.2006.01.003>
- 975 Kates, R., Turner II, B. & Clark, W. (1990). The Great Transformation in The Earth as Transformed by
976 Human Action. 1-17.
- 977 Lenton, T.,M., Held, H., Kriegler, E., Hall, J.,W., Lucht, W., Rahmstorf, S. & Schellnhuber, H.,J. (2008).
978 Tipping elements in the Earth's climate system. *Proceedings of the national Academy of Sciences*, 105(6),
979 1786--1793.
- 980 Li, J. & Roy, D.,P. (2017). A global analysis of Sentinel-2A, Sentinel-2B and Landsat-8 data revisit intervals
981 and implications for terrestrial monitoring. *Remote Sensing*, 9(9), 902.
- 982 Mildrexler, D.,J., Zhao, M. & Running, S.,W. (2009). Testing a MODIS global disturbance index across
983 North America. *Remote Sensing of Environment*, 113(10), 2103--2117.
- 984 Moffette, F., Alix-Garcia, J., Shea, K. & Pickens, A.,H. (2021). The impact of near-real-time deforestation
985 alerts across the tropics. *Nature Climate Change*, 11(2), 172--178.
- 986 Nepstad, D., McGrath, D., Stickler, C., Alencar, A., Azevedo, A., Swette, B., Bezerra, T. et al. (2014).
987 Slowing Amazon deforestation through public policy and interventions in beef and soy supply chains.
988 *science*, 344(6188), 1118--1123.

- 989 Roberts, D.,A., Gardner, M., Church, R., Ustin, S., Scheer, G. & Green, R. (1998). Mapping chaparral in the
990 Santa Monica Mountains using multiple endmember spectral mixture models. *Remote sensing of*
991 *environment*, 65(3), 267--279.
- 992 Ross, K., Brown, M., Verdin, J.,P. & Underwood, L. (2009). Review of FEWS NET biophysical monitoring
993 requirements. *Environmental Research Letters*, 4(2), 024009.
- 994 Settle, J. & Drake, N. (1993). Linear mixing and the estimation of ground cover proportions. *International*
995 *Journal of Remote Sensing*, 14(6), 1159--1177.
- 996 Shimabukuro, Y.,E., Santos, J.,a., Formaggio, A., Duarte, V., Rudorff, B., Achard, F. & Hansen, M. (2012).
997 The Brazilian Amazon monitoring program: PRODES and DETER projects. *Global forest monitoring from*
998 *earth observation*, 153--169.
- 999 Shukla, P.,R., Skeg, J., Buendia, E.,C., Masson-Delmotte, V., Portner, H., Roberts, D., Zhai, P. et al. (2019).
1000 Climate Change and Land: an IPCC special report on climate change, desertification, land degradation,
1001 sustainable land management, food security, and greenhouse gas fluxes in terrestrial ecosystems.
- 1002 Slough, T., Kopas, J. & Urpelainen, J. (2021). Satellite-based deforestation alerts with training and incentives
1003 for patrolling facilitate community monitoring in the Peruvian Amazon. *Proceedings of the National*
1004 *Academy of Sciences*, 118(29), e2015171118.
- 1005 Song, X., Hansen, M.,C., Stehman, S.,V., Potapov, P.,V., Tyukavina, A., Vermote, E.,F. & Townshend, J.,R.
1006 (2018). Global land change from 1982 to 2016. *Nature*, 560(7720), 639--643.
- 1007 Tucker, C.,J. & Nicholson, S.,E. (1999). Variations in the Size of the Sahara Desert from 1980 to 1997.
1008 *Ambio*, 28(7), 587--591.
- 1009 Ying, Q., Hansen, M.,C., Potapov, P.,V., Tyukavina, A., Wang, L., Stehman, S.,V., Moore, R. et al. (2017).
1010 Global bare ground gain from 2000 to 2012 using Landsat imagery. *Remote Sensing of Environment*, 194,
1011 161--176.
- 1012 Ying, Q., Hansen, M.,C., Sun, L., Wang, L. & Steininger, M. (2019). Satellite-detected gain in built-up area
1013 as a leading economic indicator. *Environmental Research Letters*, 14(11), 114015.

- 1014 Zhu, Z. & Evans, D.,L. (1994). US forest types and predicted percent forest cover from AVHRR data. *PE &*
1015 *RS- Photogrammetric Engineering & Remote Sensing*, 60(5), 525--531.
- 1016 MODIS VCF ATBD.